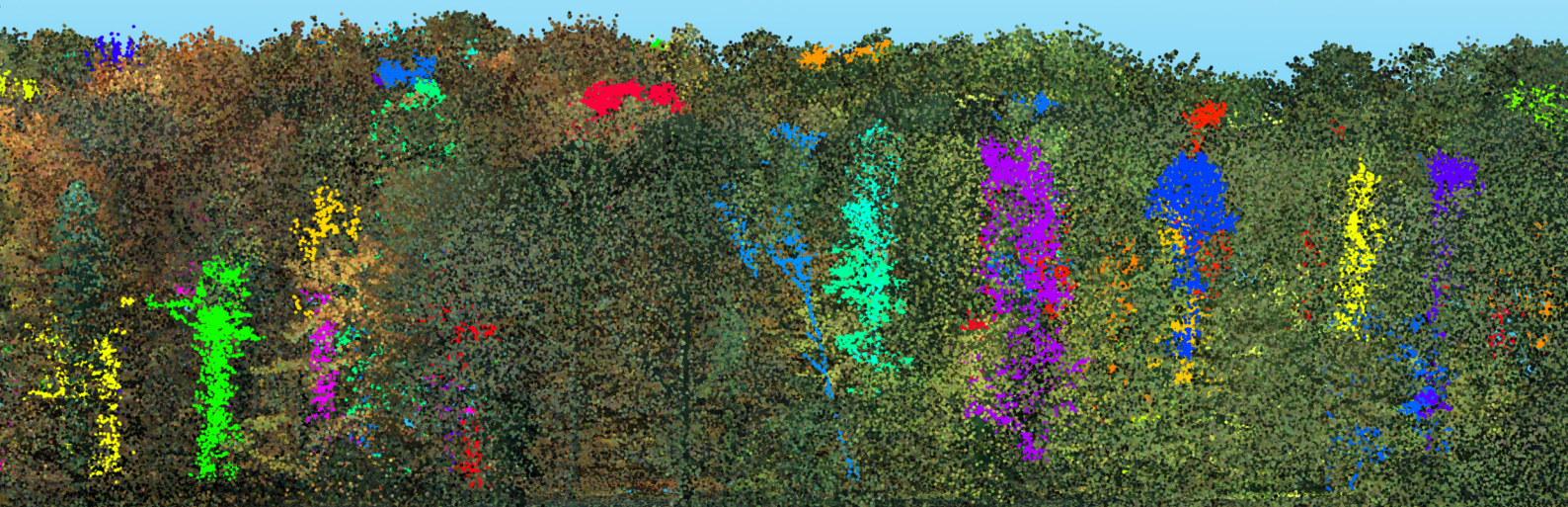


MASTER OF SCIENCE THESIS

Change Detection in Forests Using Multi-Temporal High Density Airborne Laser Scanning Data

Peter Pietrzyk

January 2015



Change Detection in Forests Using Multi-Temporal High Density Airborne Laser Scanning Data

MASTER OF SCIENCE THESIS

For obtaining the degree of Master of Science in Geomatics
at Delft University of Technology

Peter Pietrzyk

January 2015

Graduation committee:
Prof. Dr. M. Menenti, Graduation Professor
Dr. R.C. Lindenbergh, Supervisor
Drs. D.J. Dubbeling, Chair
G.A.K Arroyo Ohori, Co-reader

Delft University of Technology



Copyright © Peter Pietrzyk
All rights reserved.

Summary

Remote sensing of forests with airborne laser scanning has been used increasingly in the last decades. The reason for its success is the ability of the laser scanner to provide very detailed three-dimensional information on the structure of forests and individual trees. This makes it very suitable to detect changes in forests. However, current change detection methods can often not exploit the full potential of the information.

The increasing gap between ability of these methods and the information available in increasingly denser airborne laser scanning data has led to this research. In this thesis a method is developed that aims to use the full three-dimensional information to detect harvested and fallen trees in forests using multi-temporal high density airborne laser scanning data. The results of the method are then evaluated and finally validated based on manual extraction of trees from the data.

The method to detect harvested and fallen trees is based on the direct comparison of repeated airborne laser scanning data. In a first step, the differences between data sets are obtained through an adapted cloud-to-cloud comparison, such that the data can be reduced to the changed points only. In this way each individual point is processed and inherently the three-dimensional information can be exploited. Secondly, from the changed points the individual changed objects are extracted. This is done by first connecting points that are close together and then merging together the clusters of connected points by taking into account the shape of trees. In this way the type of each changed object can be classified as either a removed tree or another object in the final step.

The findings show that harvested and fallen trees can be detected with an overall accuracy of 65% and an omission error of 0%. The overall accuracy could be improved to 94% by adapting one parameter in the methodology. The results further indicate that smaller trees and changes below the canopy can be identified, although with lower success rates. Examples further show that small changes, e.g. removed branches, can be potentially detected. It was further shown that the high density data can be processed in a reasonable amount of time. Projected onto a square-kilometre a processing time of four hours was estimated in the longest case. All in all, it can be seen that the potential of the three-dimensional nature can be better exploited by considering each individual point of the data.

Acknowledgements

I would like to express my gratitude to my supervisor Dr. Roderik Lindenbergh for the useful comments, remarks and his engagement through the process of this thesis. Roderik further gave me the opportunity to participate at the ISPRS Technical Commission V Symposium in Riva del Garda, for which I am very grateful. It has been an insightful and priceless experience for me. Also, I especially appreciate that he never restricted me in my ideas and research.

Furthermore I would like to thank Professor Massimo Menenti for his sharp comments and supervision. Thanks as well to my co-reader Ken Arroyo Ogori, my external examiner Dirk Dubbeling and everyone at the Optical and Laser Remote Sensing section for sharing their thoughts on my thesis and providing me with valuable feedback. Furthermore I want to thank Alexander Bucksch, who shared with me his long experience in laser scanning of trees and forest and gave me valuable advice at the start of this research. Alexander is also the one to blame for my interest in remote sensing of vegetation. I am also thankful to Michiel Boelhouwer from Gemeentewerken Rotterdam for providing me with the data for this research. Without his help this research would have not been possible in this way.

I want to thank all of my Geomatics colleagues and all friends, who have supported me throughout the process of this thesis and my studies at the TU Delft. Last, but not least, I also would like to thank my loved ones, my dearest parents for their patience and encouragement and my dearest sister Monika, who has supported me emotionally the entire process. I will be grateful forever for your love.

Delft, The Netherlands
January 2015

Peter Pietrzyk

Contents

Summary	iii
Acknowledgements	v
List of Figures	x
List of Tables	xi
1 Introduction	1
1.1 Problem Statement	1
1.2 Research Question	3
2 Airborne Laser Scanning in Forestry Applications	5
2.1 Principles of LiDAR and Airborne Laser Scanning	5
2.2 Forestry Applications	6
2.3 Change Detection	8
2.4 Processing of 3D Data	10
2.5 Summary	12
3 Methodology	13
3.1 Framework of the Methodology	13
3.2 Cloud to Cloud Comparison	14
3.2.1 Degree of Change	15
3.2.2 Properties of the Degree of Change	17
3.2.3 Threshold	18
3.3 Clustering	19
3.3.1 Region Growing	19
3.3.2 Cluster Merging	20
3.4 Classification	21
3.5 Data Management and Processing	23

4	Data, Implementation and Results	25
4.1	Test Site and Data Description	25
4.2	Data Quality and Co-registration	27
4.3	Implementation	29
4.4	Sensitivity Analysis of Degree of Change	30
4.4.1	Degree of Change from 2008 to 2012	30
4.4.2	Degree of Change from 2008 to 2010	34
4.4.3	Degree of Change from 2010 to 2012	34
4.4.4	Summary	34
4.5	Detection of Harvested Trees	37
4.6	Computational Performance	40
4.7	Comparison of Results	41
4.8	Comparison to Differenced Digital Surface Models	45
4.9	Validation Based on Manual Manipulation	45
5	Conclusions and Recommendations	51
5.1	Conclusions	51
5.2	Recommendations	54
	References	57
A	Point Clouds of Sample Area	61

List of Figures

2.1	Principle of Airborne Laser Scanning.	6
2.2	Pulse returns from canopy and ground.	7
2.3	Detection of harvested trees by differencing canopy height models.	10
2.4	Construction of a kd -tree.	11
3.1	Side view of a small forest patch.	14
3.2	Cloud-to-cloud distance.	15
3.3	Principle of the robust cloud-to-cloud distance.	16
3.4	Effect of the centring procedure	17
3.5	Remaining points after application of threshold.	19
3.6	Principle of applied region growing procedure.	20
3.7	Procedure of clustering and classification.	21
3.8	Dimensions of trees.	22
3.9	Tree classification based on principal component analysis.	22
3.10	Management of tiles over a large area.	23
4.1	Aerial image of Kralingse Bos obtained in 2008.	26
4.2	Digital surface model of the Kralingse Bos.	26
4.3	Difference in elevation between 2008 and 2012.	29
4.4	Statistical relationship for comparison of 2008 data to 2012 data.	31
4.5	Statistical relationship for comparison of 2008 data to 2012 data.	31
4.6	Histogram showing effect of degree of change based classification on the basic cloud-to-cloud distance for comparison of 2008 data to 2012 data.	32
4.7	Summary of statistical relationships of multiple densities and values of k for comparison of 2008 data to 2012 data.	33
4.8	Summary of degree of change thresholds for the comparison of 2008 data to 2012 data using different values of k and densities in the reference cloud.	33

4.9	Summary of statistical relationships of multiple densities and values of k for comparison of 2008 data to 2010 data.	35
4.10	Summary of degree of change thresholds for the comparison of 2008 data to 2010 data using different densities and values of k	35
4.11	Summary of statistical relationships of multiple densities and values of k for comparison of 2010 data to 2012 data.	36
4.12	Summary of degree of change thresholds for the comparison of 2010 data to 2012 data using different densities and values of k	36
4.13	Resulting clusters after region growing.	37
4.14	Resulting trees after classification.	38
4.15	Clusters, that are classified as trees.	39
4.16	Clusters, that are not classified as trees.	39
4.17	Top view of detected trees harvested between 2008 and 2010 and between 2010 and 2012.	43
4.18	Top view of the detected trees harvested between 2008 and 2012.	43
4.19	Error due to over-segmentation of a harvested tree in one comparison.	44
4.20	Error due to over- and under-segmentation of a harvested tree in different comparisons.	44
4.21	Errors caused by different foliation states in the reference clouds.	44
4.22	Detected harvested trees shown overlaid on differences digital surface models	46
4.23	Manually extracted trees from 2012 data set.	47
4.24	Validation for detection of manually harvested trees using a threshold of 0.08 metre.	49
4.25	Validation for detection of manually harvested trees using a threshold of 1.0 metre.	49
A.1	2008 point cloud of sample area.	61
A.2	2010 point cloud of sample area.	62
A.3	2012 point cloud of sample area.	62

List of Tables

3.1	Advantages and disadvantages of choosing a large k	18
4.1	Summary of laser scanners, flight parameters and point density.	27
4.2	Validation of Z-coordinates.	28
4.3	Quality of vertical co-registration.	28
4.4	Detected harvested trees.	39
4.5	Computational performance of the method.	41
4.6	Number of points and clusters at different stages of the change detection process.	41
4.7	Comparison of detected harvested trees matched between different data pairs.	42
4.8	Summary of validation results for two different thresholds.	47
4.9	Overall accuracy and error rates for two different thresholds.	47

Chapter 1

Introduction

Today forests cover an area of 4 billion hectares, which amounts to 31% of the Earth's total land area (FAO, 2010). The detection and monitoring of changes in forests is therefore of great importance; not only because these changes are directly related to ecological aspects and climate change, but also because of the social and economic value of forests. The necessity to obtain information about forest is thus threefold. Firstly, forests host one of the richest biodiversities on Earth. They do not only consist of a wide range of different tree species but they also inhabit other living species and plants. Secondly, they are a major carbon sink and are related to climate change. Due to the photosynthetic process carbon dioxide in the atmosphere is absorbed, while with each cleared or burned tree carbon dioxide is released. Thirdly, since the dawn of civilization, forests have been an important natural resource for firewood and timber, which underlines the social and economic importance of forests. Today these aspects can be integrated under the umbrella of sustainable forest management and available monitoring data allow to further analyse these forestry management strategies. Forest managers can use that information to estimate forest growth or deforestation rates, make decisions and analyse the effect of taken measures. Overall a more sustainable way of forestry management can be achieved if forest dynamics are better understood.

In the past decades remote sensing data has been widely used for the classification of forests, to observe forest decay and health and deforestation. Next to new opportunities, which steadily improving remote sensing technologies and high quality data offer for forestry and for ecological and environmental sciences, also challenges to process and analyse these data are created. To close the gap in processing and analysis of the data and to retrieve even more information from it new methods must be developed.

1.1 Problem Statement

Changes in forest environments are caused by many natural processes and anthropogenic interventions. Natural processes range from growth, seasonal variations and competition

of individual trees for light and water to disturbances caused by insects, diseases and severe weather conditions like heavy wind gusts and snow. Anthropogenic processes include interventions such as clearing, selective removal of individual trees to improve growth of other trees and selective removal of individual branches to avoid branches falling down or to make room for paths. Due to their occurrence at different spatial and temporal scales, from small to large and from gradual to abrupt respectively, the detection and measurement of changes in forest cover and canopy structure by means of remote sensing remains a challenging task.

In contrast to data from optical sensors, which provide only two-dimensional information, airborne laser scanning (ALS) data provide information in both horizontal plane and the vertical direction. The principle of ALS is based on range measurements from an aircraft or helicopter combined with the determination of its position and attitude using a differential Global Positioning System (GPS) and Inertial Measurement Unit (IMU) (Wehr and Lohr, 1999). Modern multiple return and full-waveform laser scanners are capable of generating point clouds with densities as high as 100 points/m² and more depending on the scanner settings and flight altitude. Such scanners can provide very detailed three-dimensional information on the structure of trees and forests. If the sampling rate in the horizontal and vertical direction is sufficient to obtain a full vertical point distribution at individual tree level, this information can be used to delineate individual trees (Rahman and Gorte, 2008; Reitberger et al., 2009; Hu et al., 2014) and to extract detailed information about individual trees such as skeletons and the diameter at breast height (Bucksch et al., 2014). Likewise, by extracting the crown base height, it was shown by Popescu and Zhao (2008) that the vertical point distribution can be used to extract tree parameters below the canopy surface at individual tree level. Further, changes in forests can be detected even at low point densities by matching the histograms of the vertical point distribution from repeated airborne laser scans (Næsset and Gobakken, 2005; Yu et al., 2006). Thus, ALS data provides not only information on the canopy surface but also on the tree structure below it.

Because of this three-dimensional nature, ALS data is well suited to detect changes in forest cover and canopy structure. However, studies on changes and dynamics in forests derived from ALS data are so far still limited due to the limited amount of multi-temporal ALS datasets. In addition many of these studies use point clouds with relatively low point densities of approximately ten (Yu et al., 2004) or less points per square meter (Vastaranta et al., 2012; Vepakomma et al., 2008). Several of such studies use canopy height models (CHM), two-dimensional representations of the canopy height above the ground, to derive changes in height, to detect harvested or fallen trees and to study tree gap dynamics. The use of canopy height models is practical in most applications as it reduces the amount of data and therefore benefits simplicity and efficiency, but it does not exploit the full content of information. Smaller trees, such as suppressed or intermediate trees, might not even be represented in a canopy height model because their crowns are partly or totally covered by crowns of more dominant trees. The potential of three-dimensional ALS data to detect changes in forests is thus often not realized. It was therefore suggested to use the full height distribution of multi-temporal ALS data to detect changes in forests, such as fallen trees, defoliation and thinning, more reliably (Vastaranta et al., 2012).

In response to advancements in technology, which make high density and multi-view ALS data available, and the ineffectiveness of canopy height models to exploit the full information in ALS it becomes important to assess how all individual points can be used to detect harvested and fallen trees and possibly other changes. Similar to the efficient analysis of canopy height models the use of all data points for change detection must not be downgraded by slow and intensive processing. Since the data is of high density, efficient data structures must be used.

1.2 Research Question

Based on the problem statement the main goal of the research is to detect changes in forests and assess which data parameters are significant for this purpose. The changes that are to be studied focus on the detection of large changes such as harvested and fallen trees. Other small changes in individual trees are to be indicated only. An important aspect of the study is to use all available three-dimensional information and yet provide efficient processing methods. Resulting from the problem statement and goal the main research question of this thesis can be defined:

How can changes in forests be detected efficiently and reliably using high density ALS data?

In order to highlight the main aspects, the research question is subdivided into four sub-questions.

1. *How can differences between multi-temporal ALS data be detected in the three-dimensional space?* This question focuses on the extraction of differences between two or more co-registered ALS point clouds of the same area. The proposed methodology has to work in the three-dimensional space. Differences due to the measurement, such as measurement noise, point density variations and sub-sampling, should also be considered.
2. *How can harvested and fallen trees in forests be extracted from differences detected between multi-temporal ALS data?* Differences between the data sets can occur due to several reasons. The objective here is to extract physical changes in the forest that occurred between the acquisitions. In particular, the focus is on the extraction of harvested or fallen trees.
3. *What is the computational performance to extract these changes?* To develop and use an efficient method is a goal of the research. To evaluate the efficiency of the used methods and algorithms the amount of computational resources required for individual parts of the proposed methodology must be analysed.
4. *How can the detected changes be validated?* The quality of the results must be verified in the end. Here the aim is to determine how accurate the results are in comparison to findings from field work or visual interpretation of the data. Further it has to be evaluated how sensitive the outcomes are to variables like point density or method parameters. This sub-question deals with the quality assessment of the results.

Certain limitations to the research are presented in order to focus the scope of the study. The research aims at finding differences directly from the data. This means that inferring variables like trunk volume, diameter at breast height, biomass from the data and subsequently comparing these variables between different years is beyond the scope of this research. Further, even though the research is aiming at developing an efficient method it is not the goal to fully optimize the implementation of the method for speed and memory usage. Lastly a detailed accuracy assessment of the results is not possible because no in situ data is available and is thus beyond the scope of the research.

Airborne Laser Scanning in Forestry Applications

In this chapter the theoretical background of airborne laser scanning in forest environments as well as an overview of previous research on the topic are given. The basic technical principles of airborne laser scanning are discussed in Section 2.1. Next, an overview of the usage of airborne laser scanning in forest environments, the interaction of the laser and the forest, and the extraction of forest variables is presented in Section 2.2. Further, Section 2.3 shows state-of-the-art research on change detection in forests using airborne laser scanning data. New approaches to detect changes from laser scanning data in the three-dimension space are described in Section 2.4. Finally, Section 2.5 concludes with a summary of the problems with current methods.

2.1 Principles of LiDAR and Airborne Laser Scanning

Airborne laser scanning (ALS) is an active remote sensing technique that measures the elevation of an area from a fixed wing aircraft or a helicopter (Figure 2.1). The two main components of an ALS system are a laser scanner, which takes range measurements to the ground at a high frequency, and a combination of differential GPS and an inertial measurement unit (IMU), which determines the position and orientation of the flying platform. Together they produce the absolute position of the measured points.

ALS systems use mainly pulse lasers, which measure the time-of-flight of a pulse, i.e. the period between the emission of the pulse and the return of its echo. Knowing the speed of light the range can be computed from the time-of-flight. Further, modern laser scanners are capable of capturing more than one peak in the echo of a single pulse, which due to the divergence of the laser beam can occur if multiple objects are hit. For a discrete return laser scanner the peaks result in a discrete and finite number of points, that correspond to the first, the last or an intermediate peak in the echo. Full-waveform scanners on the

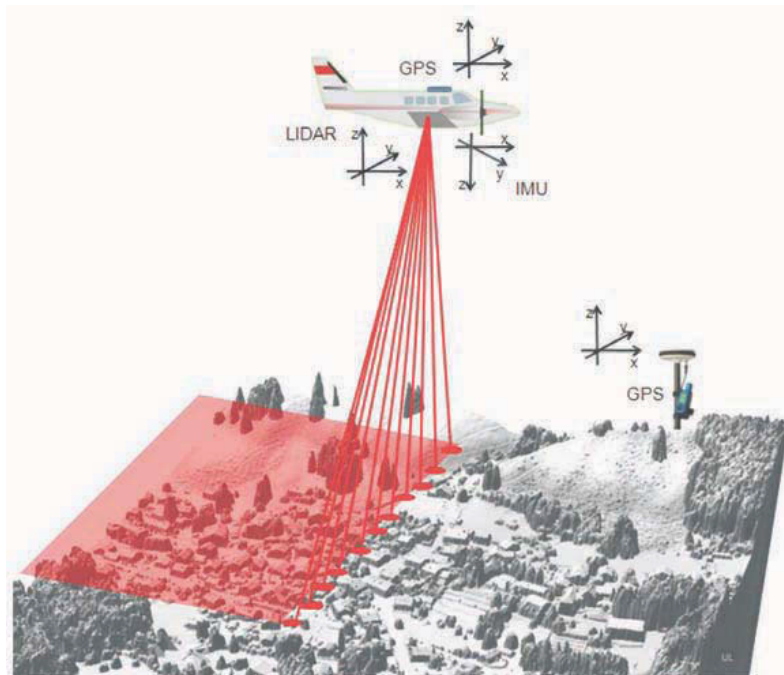


Figure 2.1: Principle of Airborne Laser Scanning. Source: [Vosselman and Maas \(2010\)](#)

other hand return a continuous measurement of the received intensity of the echo. This waveform can be processed directly or discrete points can be extracted from the waveform.

Due to the movement of the scanner across-track and the movement of the platform along-track a large number of points can be scanned over a large area resulting in high density 3D point clouds. The used ALS system and the flying altitude and speed all influence the resulting point density, such that at higher flying altitudes and faster flying speed the point density is reduced. Depending on these parameters the point densities can be as high as 100 points/m² or more. Further overlapping flight-strips, scan angle and largest possible number of returns have a large impact on the density and variations in density. For a more extensive overview about ALS the reader is referred to [Shan and Toth \(2008\)](#) and [Vosselman and Maas \(2010\)](#).

2.2 Forestry Applications

The capability of ALS systems to capture more than one pulse echo can be exploited in forest environments. A scanner, which captures the first and last returned echo of a pulse, would most likely receive the first pulse from the top of the canopy and the last pulse from the ground. The latter is made possible by the ability of the laser pulses to penetrate through the porous canopy. As illustrated in [Figure 2.2](#) a scanner, that captures more than the first and last returns, or yet a full-waveform scanner, can in addition capture echoes from the vegetation in between the canopy surface. This results in information about the horizontal and vertical distribution of vegetation in the forest and makes ALS therefore particularly useful for forest environments.

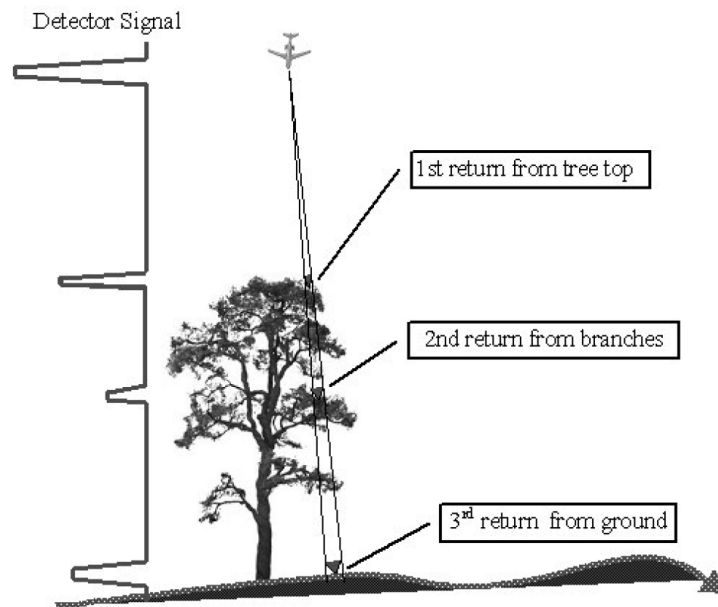


Figure 2.2: Pulse returns from canopy and ground. Source: Yu (2008)

Research on the use of the LiDAR technology for forestry applications dates back to the early 1980s using LiDAR profilers (Lim et al., 2003). By the 1990s, due to developments in GPS and IMUs, modern small footprint laser scanners were used already for topographic mapping and a little later also in forestry (Hyypä et al., 2008). First research concentrated on the generation of Digital Terrain Models (DTM), which correspond to the elevation of the bare earth points. This is possible when a laser pulse penetrates the porous canopy and is then reflected from the ground surface. Subsequently the generated digital terrain model can be used to estimate the height above ground of other non-ground points. In combination with a Digital Surface Model (DSM), corresponding to the top of the canopy, the digital terrain model can be used to generate a Canopy Height Model (CHM), representing the height of the canopy surface above the ground and thus tree height. Because the point density and beam divergence are directly related to the spatial coverage of the sensed area and because they are usually insufficient to provide a continuous spatial coverage, any scanned object must be considered to be undersampled. This is more severe in the vertical than in the horizontal direction and can be explained by the scanning being done from above the forest. In particular this is caused by the incidence angle of the laser pulse and the objects, i.e. the scanning geometry, and the penetration rate of laser pulses through the canopy. Therefore the vertical distribution of points must be expected to be coarser in the vertical direction. The undersampling in the horizontal plane often results in missed treetops and therefore an underestimate in tree height as mentioned by Vosselman and Maas (2010) and Hyypä et al. (2008). They further summarize the factors which affect tree height underestimation: tree bending due to wind; penetration rate of laser pulses into the crown; ground vegetation influencing the generation of the digital terrain model and the used algorithms; the laser system and signal processing; and the tree shape and species.

In order to extract forests and tree attributes from ALS data two approaches have emerged (Vauhkonen et al., 2014; Hyyppä et al., 2008), namely area-based methods and individual-tree-based methods. Area-based methods, alternatively called distribution-based methods, focus on extracting metrics from the vertical distribution of points within an area of adequate size, such as grid cell plots with widths in the order of tens of meters (i.e. larger than the crown diameter) or full stands. Here only the vertical component, i.e. height above ground, of the measured points is considered and the horizontal distribution within the grid cell or plot is neglected. From the vertical distribution a number of parameters, such as different height percentiles, can be extracted and with regression analysis related to forest attributes, like mean stand or plot height, biomass or mean diameter at breast height (DBH).

The second approach uses individual-tree-based methods. The focus here is on the extraction of parameters of individual trees and the estimation of attributes using allometric relations. The general process includes individual tree detection (ITD), feature extraction and the estimation of tree attributes (Vauhkonen et al., 2014). Extractable features can include the tree position, tree height, crown dimensions and intensity distributions. Tree attributes to be predicted from these features could be DBH, timber volume or biomass. The detection of individual trees can be done in several ways with varying success rates depending on the used algorithm and the data and site specifications (Vauhkonen et al., 2011; Kaartinen et al., 2012; Wallace et al., 2014). This might fail in two ways: a tree can remain undetected, resulting in an omission error, or false trees can be produced, resulting in commission errors. Many of the ITD methods are based on canopy height models and use watershed segmentation, slope based or edge detection algorithms to delineate tree crowns. A significant drawback of canopy height model based approaches is that smaller trees, whose crowns are partly or completely suppressed by crowns of neighbouring trees and therefore do not appear in the canopy height model, are difficult or impossible to detect. Other methods are based on individual points or a gridded voxel space. Morsdorf et al. (2003) presented an approach using k-means clustering of all individual points in the data and used the local maxima in the digital surface model for seed point selection. In a study by Reitberger et al. (2009) a normalized-cut approach was used to delineate a voxelized point cloud. Lee et al. (2010) presented a adaptive clustering approach, which uses agglomerative clustering of super-segments that were already created using region growing beforehand. However, regardless of the algorithm, data and site characteristics it must be expected that not all trees can be extracted from the point cloud. In addition, the actual tree height is often underestimated in ALS based tree height assessments due to undersampling, which can only be partly corrected by regression models (Leeuwen and Nieuwenhuis, 2010).

2.3 Change Detection

Monitoring of changes in forests using ALS data is a relatively new field of science. Since the first papers on the topic were published in 2004 only a small amount of research has been conducted due to the limited number of available multi-temporal ALS data sets acquired over forest environments. McRoberts et al. (2014) gives an overview of the studies that have been conducted upto this time and categorized them into individual-tree

and area-based studies, which in essence use the same approach as explained in Section 2.2. In addition, studies on canopy gaps are considered. These are in between individual-tree and area-based studies and focus on the measurement of the dynamics of gaps in the canopy, such as creation of new gaps, expansion and closing of existing gaps. McRoberts et al. (2014) further distinguishes between the direct method, in which "change in the variable of interest is estimated directly from multi-temporal auxiliary data such as ALS height and density metrics", and the indirect method, in which "change is estimated as the difference between estimates of the variable at two points in time".

Parametrizing changes in forest can be a complicated task, because there are different processes responsible for change, which include vertical and horizontal growth of crowns, seasonal variations in needles and leaves, the state of undergrowth and low vegetation, and the movement of trees caused by wind (Hyypä et al., 2008). Additionally, the ability to monitor logging activities and degradation in forests can be disturbed by re-vegetation of the canopy. This list can be complemented by the factors stated in Section 2.2, like point density or beam divergence, which influence the measured tree height. For individual-tree based studies it has to be further considered that omission and commission errors of the ITD process can differ between two acquisitions and therefore can cause an accumulation of errors (McRoberts et al., 2014).

For estimation of tree growth a range of approaches has been used, including individual-tree and area-based methods, as well as direct and indirect approaches. For detection of harvested trees or damages and modelling of canopy gap dynamics several studies have focused on the use of canopy height models and a few used area-based methods. Yu et al. (2004) automatically detected 61 out of 83 harvested trees by differencing canopy height models from 1998 and 2000 data with densities of 10 points/m². After applying a threshold to the difference in height, a filter was applied and individual trees were segmented (see Figure 2.3). The method successfully detected all mature harvested trees, but could not detect small trees. Further, difficulties to correctly segment harvested tree groups (in particular deciduous) have been observed, leading to both omission and commission errors. In a series of studies, Vepakomma et al. (2008, 2010, 2012) used canopy height models to identify and classify canopy gap dynamics into groups such as creation of new gaps, gap expansion, and laterally and vertically closing gaps. Vastaranta et al. (2012) differenced canopy height models of 2006 and 2010 to map snow induced canopy damage by applying a threshold on the difference in height and setting a minimum area requirement. The best set of parameter yielded rates of omission errors between 19% and 75% per plot and rates of commission errors between 0% and 25%. It was concluded that the method is only suitable for dominant and codominant trees if dense point cloud data is available. By using height distributions in 5 x 5 meter grid cells it was shown previously that cells with damaged trees could be detected with an overall accuracy of 78.6% (Vastaranta et al., 2011) and therefore suggest to be superior over an approach based on canopy height model. Nyström et al. (2013) demonstrated that areas with no harvested trees, 50% of the trees removed and 100% of the trees removed can be successfully classified with an overall accuracy of 88% by using an area-based approach. In the study height and density metrics in 10 x 10 meter grid cells have been derived from two separate acquisitions and calibrated against each other using histogram matching in order classify individual grid cells more accurately.

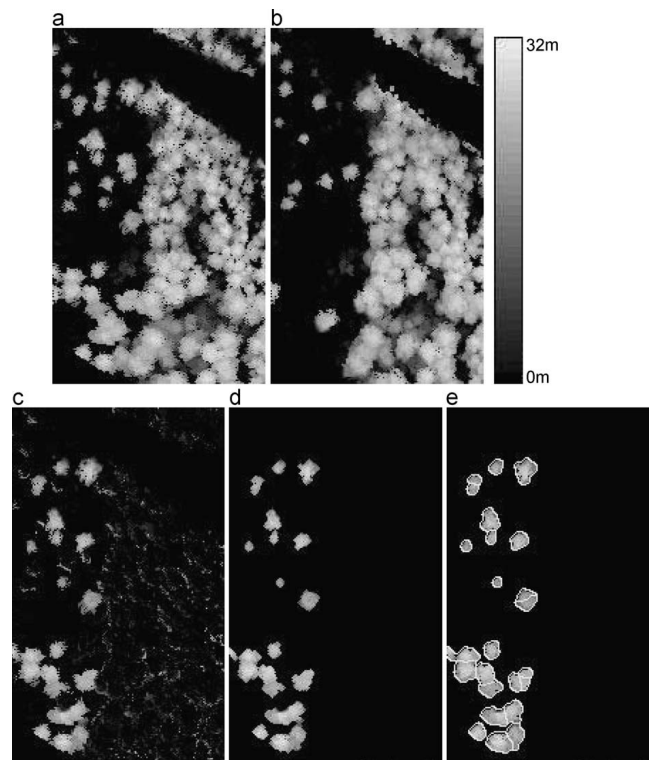


Figure 2.3: Detection of harvested trees by differencing canopy height models. (a) CHM of 2008, (b) CHM of 2010, (c) differenced CHMs, (d) after applying threshold and filter and (e) segmentation of individual harvested trees. Source: Yu et al. (2004)

2.4 Processing of 3D Data

A number of studies have explored the potential of comparing point clouds in all three dimensions and on the individual point level. The underlying principle is that data structures are used to spatially partition the raw point cloud in order to make the comparison of point clouds efficient. Comparisons can be then performed by comparing either the spatial partitions or individual points. Girardeau-Montaut et al. (2005) used sets of terrestrial laser scanning data with diverging point densities to detect changes using octree structures. It was concluded that either a fast process can be used for preview or a more precise but slower comparison relying on a point-to-point based approach. Barber et al. (2008) organized point clouds in octree data structures and compared nodes of the octrees to each other and points to nodes in order to identify significant changes between two sets of point cloud data. Both studies further addressed the problem that registration errors of multi-temporal data sets may affect the results. Richter et al. (2013) compared point clouds based on a point-to-point approach using octrees to structure point clouds and improve computing time. Similarly to Girardeau-Montaut et al. (2005) the study relied on the computation of the distance of each point in one point cloud to its nearest neighbour in a second point cloud. Here the former point cloud is called the *compared cloud* and the latter the *reference cloud*. The result is a cloud-to-cloud distance, which is attributed to each point in the compared cloud and which can indicate changes. As

shown by Girardeau-Montaut et al. (2005) and Richter et al. (2013) a low value of this distance indicates that no change has occurred, while a large value indicates that there has been a change. Nevertheless the results are sensitive to the sampling density, occlusion of objects and the distance does not necessarily correspond to real changes (Girardeau-Montaut et al., 2005). It was already shown that a similar approach can be used in forests to obtain most changes in the three-dimensional structure between the terrain and the canopy surface (Lindenbergh and Pietrzyk, 2015). In Pietrzyk and Lindenbergh (2014) it was shown that an adapted approach can be used to automatically identify removed trees in forests from bi-temporal ALS data.

In the simplest way the nearest neighbour of a point could be found by calculating the distance to all other points and then identifying the point corresponding to the smallest distance. This can be extended to finding the k nearest neighbours or all neighbours within a certain range. If one wants to find the nearest neighbours of each point, this brute force approach has a quadratic complexity $O(n^2)$, where n is the number of points, and is thus not efficient for large data sets. By using a spatial data structure the search can be limited to the points in the vicinity of the query point and the computation time can be reduced considerably. A data structure, other than the octree structure mentioned above, that can be used for this is the kd -tree (Friedman et al., 1977). This method is used in this study and is explained here with a 2D case. A kd -tree is a binary search tree that partitions the data according to the distribution of the data. In this way it takes into account the local density of the data, such that in denser regions the partitions are finer. Figure 2.4 illustrates the construction of a kd -tree. At the starting node the data is split into two nodes along the dimension with the largest spread and at the median value. Next, both nodes are treated separately and split again in the same manner as before. This is continued until each node contains a maximum number of points, in this case one point. The resulting tree is build with a complexity of $O(kn \log n)$, where k is the number of dimensions and n the number of points.

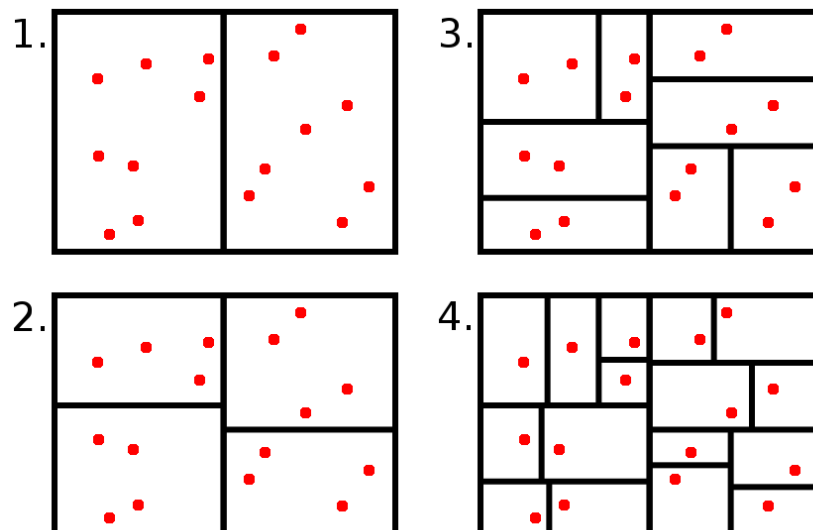


Figure 2.4: Construction of a kd -tree.

After the construction of the kd -tree it can be used to find the k nearest neighbours of a query point. Therefore, as the first step, the leaf node that corresponds to the query point is determined. This is done by traversing the tree until a leaf node is reached. Then the closest k points in that node and their distance to the query point are determined. If other leaf nodes are within the same distance to the query point as the k th closest points, they are inspected for points that are closer than the previously determined ones. Proceeding in this way only a small subset of the whole data has to be searched for the k nearest neighbours instead of the whole data set. In most cases the complexity to find the k nearest neighbours is proportional to $\log n$.

2.5 Summary

It has been shown that ALS has many advantages for the analysis of forests. Due to its three-dimensional nature and its capability to penetrate the porous canopy, information about the vegetation structure at the canopy surface and below it can be obtained. Current methods however do not fully exploit this potential as they either consider the canopy surface only or take averages over larger areas. Further, methods that look at individual trees suffer from errors obtained during the delineation of individual trees. The result of these approaches is that in particular changes below the canopy surface cannot be detected.

Other approaches that do consider the three-dimensional nature of laser scanning data suffer from the fact that they detect differences between multi-temporal data rather than real changes. The reasons for this are due variations in the sampling density and occlusion. So far research on this topic in forests has only been done by [Pietrzyk and Lindenbergh \(2014\)](#), which was part of this thesis work. This research is completed with this thesis report.

Methodology

In this chapter the workflow and methodology to meet the objectives of this research are described. First, an overview of the methodology and algorithms together with their requirements is given in Section 3.1. Then, sections 3.2, 3.3 and 3.4 explain the individual steps of the developed methodology to detect harvested or fallen trees. Because of the large amount of data it is proposed to manage the point cloud files as described in Section 3.5 in order to process a larger area.

3.1 Framework of the Methodology

Based on the research goals two important requirements can be set for the detection of changes in forests from bi-temporal ALS data. First, the method has to utilize the full three-dimensional nature of the data, and secondly, it has to be computationally efficient. In addition, effects on the data which result from the geometrical structure of forest, the scanning process or their combination must be dealt with.

In essence the spatial distribution of points depends on the object geometry. The distribution can be volumetric, e.g. in tree crowns or undergrowth, or planar at the ground surface, or linear at trunks and branches. In addition, the scanning process results in variations in the point distribution due to different incidence and scan angles, overlapping strips, maximum number of returns, the sensitivity of the laser scanner and other factors. Measurement noise, point density, occlusion, and the obvious but substantial fact that any object is sub-sampled further affect the point distributions and cause differences between multi-temporal ALS data sets. While these effects cannot be eliminated completely they do have to be taken into account.

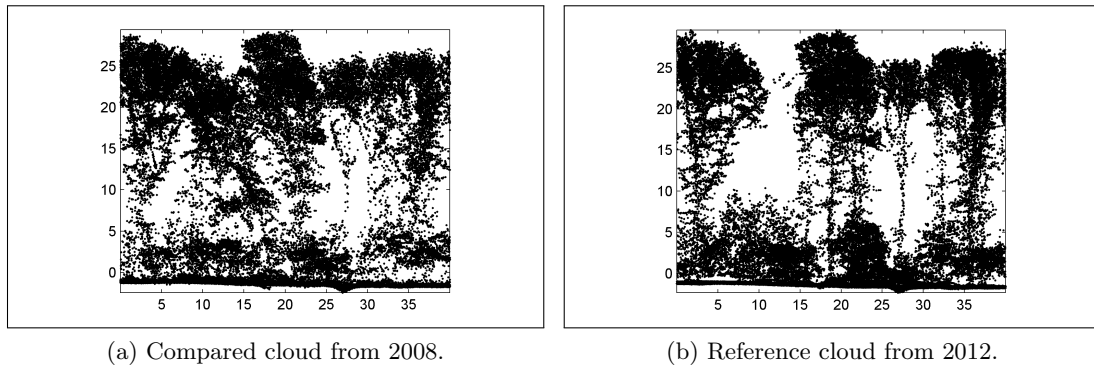


Figure 3.1: Side view of a small forest patch.

The basic idea of the method is based on a direct comparison of the raw point clouds with subsequent segmentation and classification. The process is therefore divided into three components:

1. Deviating points are determined individually using a modified cloud-to-cloud comparison, which identifies differences between the data sets.
2. The deviating points are further clustered into spatially connected regions.
3. The clusters are classified into either trees or other objects like undergrowth or noise.

The individual steps of the research methodology are illustrated with a small forest patch as running example. Figure 3.1a shows the point cloud of this forest patch acquired in 2008 and Figure 3.1b the corresponding point cloud acquired in 2012. A visual comparison of the two patches quickly reveals the removal of trees between the acquisitions of both data sets, but also small differences in the canopy and undergrowth can be observed.

3.2 Cloud to Cloud Comparison

As was shown in Section 2.4 changes between two data sets can be detected on an individual point basis by computing the distances for all points in one data set to their respective nearest neighbours in the other data set. An example of this is illustrated in Figure 3.2, where points in the first data set, which belong to a tree that exists in the first data set but not in the second, will have a large distance. For these points the closest points in the second data set will in fact belong to structures that still exist, like the ground or neighbouring trees, which, however, might be far away.

Nevertheless, due to adverse characteristics of the point distribution, which are caused by a combination of the object geometry and the scanning process, this cloud-to-cloud distance necessarily suffers from a low signal-to-noise ratio. The cloud-to-cloud distance is thus not only the result of changes but other factors, too. For example, the cloud-to-cloud distance at a tree trunk is, due to the low sampling, in general larger than for ground

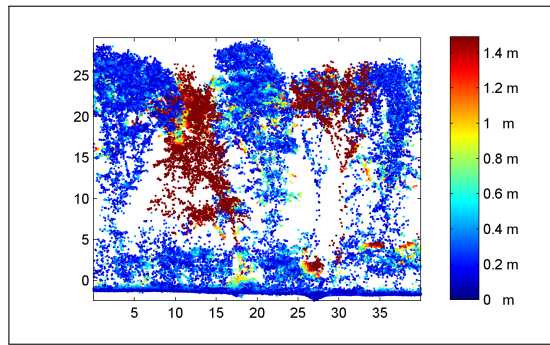


Figure 3.2: Cloud-to-cloud distance. Distance to the nearest neighbour in reference cloud.

points. Such differences result in an essential problem. It is not obvious which cloud-to-cloud distance can be regarded as a change, and above that there is inevitably an overlap in the distances that can be considered to be related to changes and the distances that can be considered to be related to similarities. It is therefore required to compute the amount of change in an alternative manner such that a unique threshold can be applied, which separates changed from non-changed points.

3.2.1 Degree of Change

To resolve the described problems two modifications are made to the cloud-to-cloud distance and are illustrated in Figure 3.3, where point A is the query point in the compared cloud and points B, C and D are points in the reference cloud:

1. **The mean of the distances to the k nearest neighbours is calculated, where k is a user defined integer.** In Figure 3.3 this is the mean of the distances of point A to B, C and D, indicated by the red circle. Even though this distance automatically increases for all query points when k is increased, it gives a more robust measure of differences between the data sets. In this way outliers, which could be caused by measurement errors, occlusion, varying point densities, small effects due to wind or small changes, are better handled. For the remainder of this paper we henceforth call this distance the robust cloud-to-cloud distance of order k .
2. **The distances between points in the reference cloud are used to calculate the degree of change.** This is done as follows. For the k nearest neighbours in the reference cloud (in Figure 3.3 points B, C and D) their individual k nearest neighbours in the reference cloud are identified and the mean of their distances is calculated. The result is a set of k distances and in the example they are indicated by the blue, green and pink circles. The mean of these k distances defines the degree of isolation that is subtracted from the robust cloud-to-cloud distance to obtain the degree of change.

The derived degree of change can then be summarized with Equation 3.1. The first part of the right-hand side is the robust cloud-to-cloud distance, where d_j is the distance from

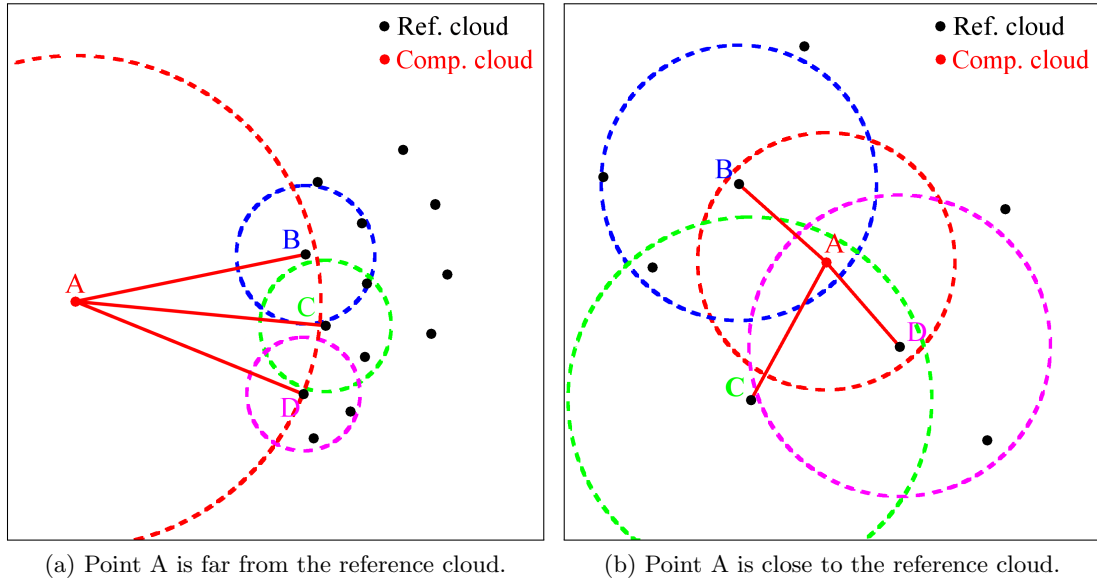


Figure 3.3: Principle of the robust cloud-to-cloud distance.

the query point A in the compared cloud to the j th nearest neighbour (B,C or D) in the reference cloud. The second part of the right-hand side is the degree of isolation, where d_i^j is the distance from the j th nearest neighbour (B,C or D) of the query point to its own i th nearest neighbour.

$$D_k(A) = \frac{1}{k} \sum_{j=1}^k d_j - \frac{1}{k^2} \sum_{j=1}^k \sum_{i=1}^k d_i^j \quad (3.1)$$

Figure 3.3 shows two cases, one where the compared point A is far from the reference cloud and one where the compared point A is close to the reference cloud. It can be seen that in the first case the robust cloud-to-cloud distance, i.e. the radius of the red circle, is larger than the degree of isolation, i.e. the mean of the other three circles. The degree of change is therefore larger than zero and point A can be considered to have changed. In the second case the opposite can be observed and point A cannot be considered to have changed. The individual components to compute the degree of change and the final results are further shown for the running example in Figure 3.4. Due to the large values the robust cloud-to-cloud distance in Figure 3.4a already gives a good indication of the trees that have been removed. In addition it can be observed that objects that have not changed still differ in that value, in particular the ground compared the other objects. The same is observed in the histogram in Figure 3.4e. Figure 3.4b shows the mean distances between the points in the reference cloud, which are then projected onto the compared cloud in Figure 3.4c. Here in particular the effect of point density in the reference cloud on the data comparison can be observed. The final degree of change is shown Figure 3.4d and the histogram in 3.4f. Indeed not changed points are centred around zero and changes are larger than zero.

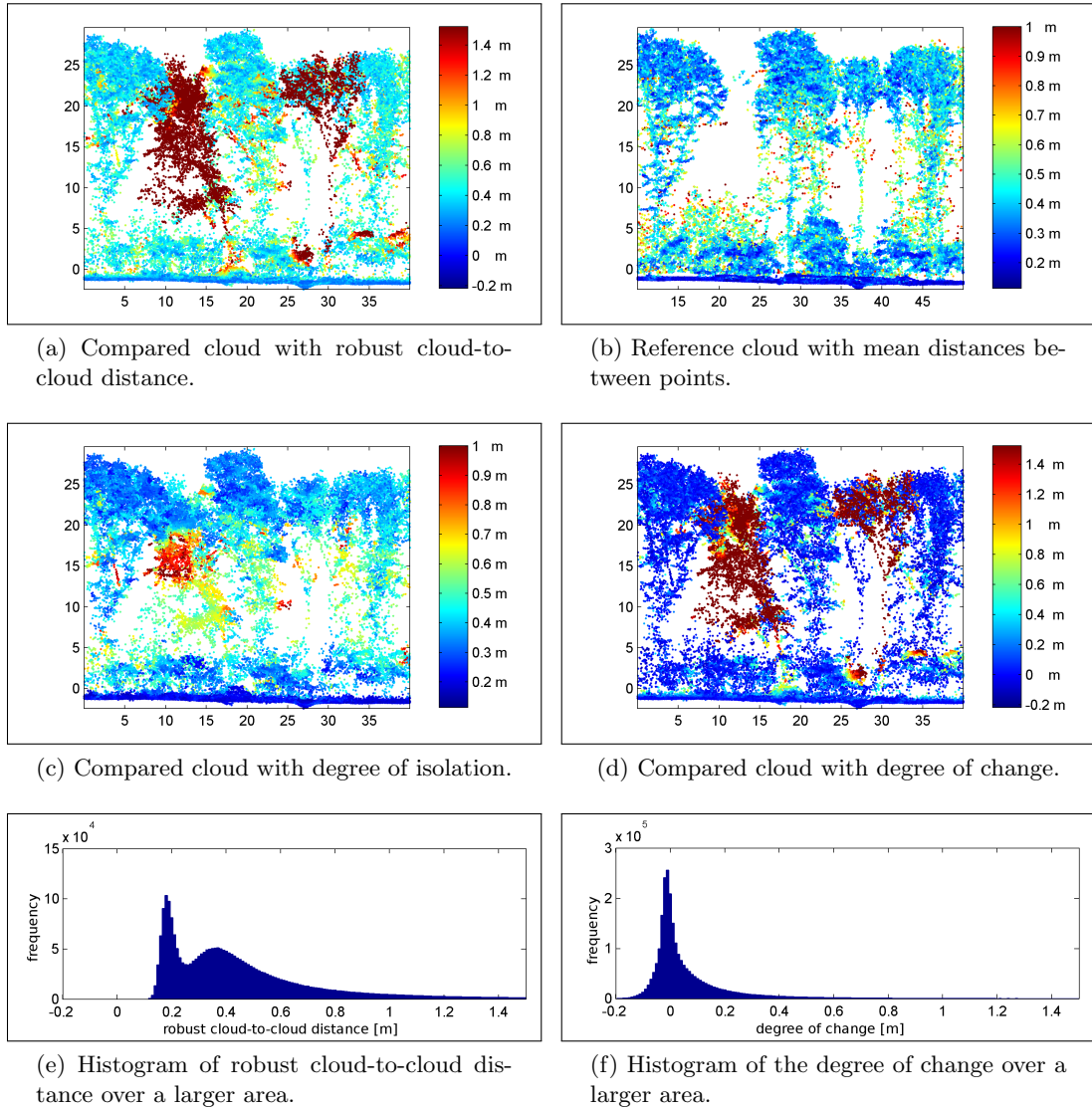


Figure 3.4: Effect of the centring procedure on the robust cloud-to-cloud distance.

3.2.2 Properties of the Degree of Change

The choice of the parameter k has several effects on the obtained degree of change. With a larger value of k the influence of irregularities on the degree of change is reduced and the decision can be based on a larger amount of information, however only at the cost of processing efficiency. If k is taken too big the advantage of analysing only the local space around the query point might however get lost. The advantages and disadvantages of choosing a larger k are summarized in Table 3.1.

Next to these properties, the degree of change has the essential characteristic that in principle the result for one value of k can be compared to results for another value of k , i.e. k does not bias the outcome. This is because the distance from the query point to its k th nearest neighbour is centred by the mean of all k th nearest neighbours in the

Table 3.1: Advantages and disadvantages of choosing a large k

Advantages	Disadvantages
<ul style="list-style-type: none"> • Reduction of noise • More statistical information available • Lower sensitivity to small changes in k 	<ul style="list-style-type: none"> • Influence by too far objects increases and effect of locality might be lost • Computational load • Increased memory usage

reference cloud as shown in Equation 3.2. Taking the mean for all k gives then Equation 3.3, which is equivalent to the degree of change in Equation 3.1.

$$\tilde{d}_j = d_j - \frac{1}{k} \sum_{i=1}^k d_i^j, \{j \in \mathbb{Z} \mid 1 \leq j \leq k\} \quad (3.2)$$

$$D_k = \frac{1}{k} \sum_{j=1}^k \left[d_j - \frac{1}{k} \sum_{i=1}^k d_i^j \right] \quad (3.3)$$

3.2.3 Threshold

To separate changes from non-changes a threshold is defined for the degree of change, such that points with a value above this threshold are classified as change. All remaining points are not considered to be changes and belong to the same object in the reference epoch. This threshold is obtained from the whole set of degrees of change obtained over a larger area and is equal to 1.5 times the interquartile range IQR above the third quartile Q_3 (see Equation 3.4). This ensures that the threshold is not affected by significant changes but rather determined by the majority of degrees of change, i.e. values that are close to zero and that can be regarded as not being a change or a minor change. In addition it has the effect that changes in foliation can be disregarded when searching for large changes such as harvested trees. After applying the threshold obtained from the distribution in Figure 3.4f the remaining points can be seen in Figure 3.5.

$$Threshold = Q_3 + 1.5 * IQR \quad (3.4)$$

Summarized it can be said that this method is purely density based, because it only takes into account the spread between points. It does not consider the shape and orientation of the point distribution in the reference cloud nor does it consider how the query point relates to that shape and orientation. Consider for example the difference between a query point with respect to a planar (e.g. ground surface) and a query point with respect to a volumetric (e.g. tree crown) point distribution. While this difference has an effect on the resulting degree of change it is not taken into account explicitly. Further the degree of

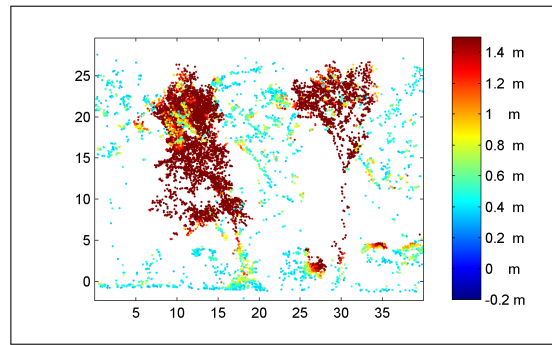


Figure 3.5: Remaining points after application of threshold on the degree of change.

change is not symmetric. Calculating it from a point cloud PC_1 to point cloud PC_2 gives a different result than calculating it from point cloud PC_2 to point cloud PC_1 . This is actually a feature of this method because it makes it possible to detect removed objects by computing the degree of change from a point cloud of a particular year to a point cloud of a later year. Calculating it from a point cloud of a particular year to a point cloud of an earlier year on the other hand would result in the detection of growth.

3.3 Clustering

In order to extract single trees the identified deviating points must be segmented. Two characteristics of the change detection procedure distinguish this approach from other approaches to delineate individual trees. First, most harvested trees are isolated harvested trees, and secondly, the data is filled with a large amount of small clusters or individual points belonging to small changes. In order to deal with these aspects of the data the tree extraction is divided into two components. First clusters of points are formed using region growing. This will result in an over-segmentation of trees. Next, the clusters are merged to form either complete trees or other clusters.

3.3.1 Region Growing

The first step clusters points into spatially connected regions using region growing. Region growing is used with the point having maximal height as initial seed. Starting from this seed the cluster is grown to candidate points, if several criteria are satisfied until all candidate points are added to the cluster. This procedure is stopped when no more candidate points are available for that particular cluster. Subsequently a new cluster is grown from the remaining points starting again at the point having the maximal height as seed. This is iterated until no more points are available as seeds. To limit the growing only close-by neighbouring points are used as candidate points. These are defined as the k nearest neighbours in the set of all points, which are identified as change, and that are within a distance of one meter to the seed. The value of k here can be different than the value used for the calculation of the degree of change in Section 3.2.

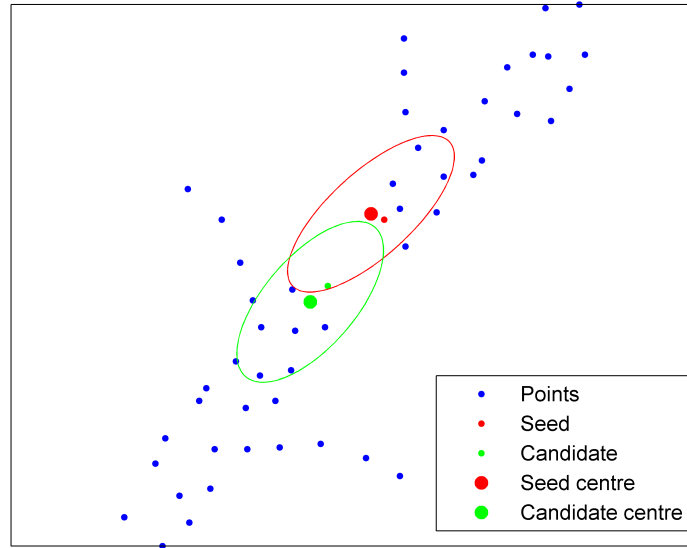


Figure 3.6: Principle of applied region growing procedure.

Further the seed point and the candidate point must satisfy a connectivity criterion. The centroid and the covariance matrix of the x , y and z coordinates of the k nearest neighbours of the seed point and the seed point itself describe the local space around a seed point as shown as large red point and ellipse in Figure 3.6. Based on this information the Mahalanobis distance to that space can be computed for any point as given by Equation 3.5, where x contains the coordinates of a point for which the distance is computed, μ is the centroid and S the covariance matrix.

$$D_{mah}(x) = \sqrt{(x - \mu)^T S^{-1} (x - \mu)} \quad (3.5)$$

Rather than taking the distance to the candidate point, the distance is calculated to the centroid of the k nearest neighbours of the candidate point and the candidate point itself, shown as large green point in Figure 3.6. This is preferred because the two centroids are further away the more disconnected the seed and candidate points are. If there is a strong connection on the other hand the centroids are closer together. Additionally, the Mahalanobis distance is calculated vice versa using the covariance matrix formed by the space around the candidate point. By setting a upper threshold on the resulting two distances the region growing process can be influenced, with a smaller value leading to smaller clusters and larger value leading to larger clusters.

3.3.2 Cluster Merging

In a similar way as in Lee et al. (2010) the obtained clusters are subsequently merged using a bottom-up approach. Here, however two clusters are merged if the horizontal distance between their centroids is the smallest distance between all cluster centroids and if these two cluster are connected. Connectivity here means that at least one point in

one cluster is the k nearest neighbour of a point in the other cluster and their distance is smaller than one meter. In this way not all clusters can be merged immediately even if their horizontal distance is small. Further, computational requirements are reduced because not all possible horizontal distances between all clusters have to be computed and stored. The benefit of this approach is that the clusters that fit together best are merged first. Clusters are merged until a threshold for the horizontal distance is reached. This threshold must be site specific, because a large value will merge two trees if it is too large and over-segment trees if too small. A value smaller than the distance between tree trunks and larger than the crown radius should be taken. The result of the merged clusters for the changed points is given Figure 3.7a.

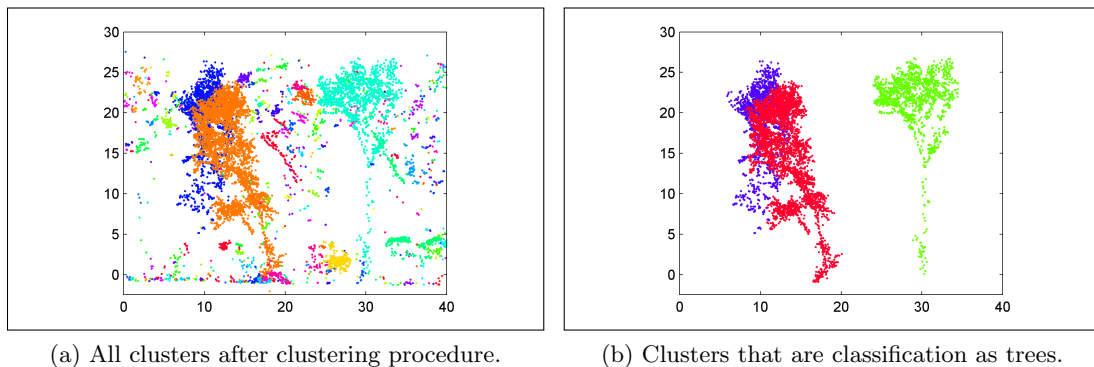


Figure 3.7: Procedure of clustering and classification.

3.4 Classification

In the final step to detect harvested trees the clusters are analysed to identify whether they are in fact trees or other objects (see Figure 3.7b). Clusters that satisfy the following three requirements for the tree dimensions (see Figure 3.8) are classified as trees.

1. The minimum tree height is 10 meters and is measured as the height above ground of the highest point.
2. The vertical expansion, i.e. distance between the lowest and highest point, must be at least 5 meters.
3. The vertical expansion must be larger than the horizontal expansion.

In this way clusters that are undergrowth, parts of trees like small parts of crowns or branches, are excluded. On the other hand, complete trees, trunks and dead trees without crowns can be classified as trees. Also in the case of over-segmentation of the tree into crown and trunk and in the case of severe under-sampling of the trunk the clusters can be still classified as trees if they meet the given requirements. In this case both clusters would be wrongly identified as individual trees.

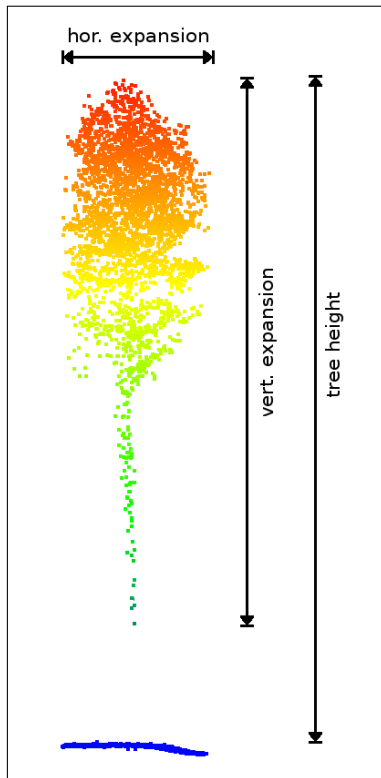


Figure 3.8: Dimensions of trees required for classification indicating the tree height, horizontal and vertical expansion of the tree.

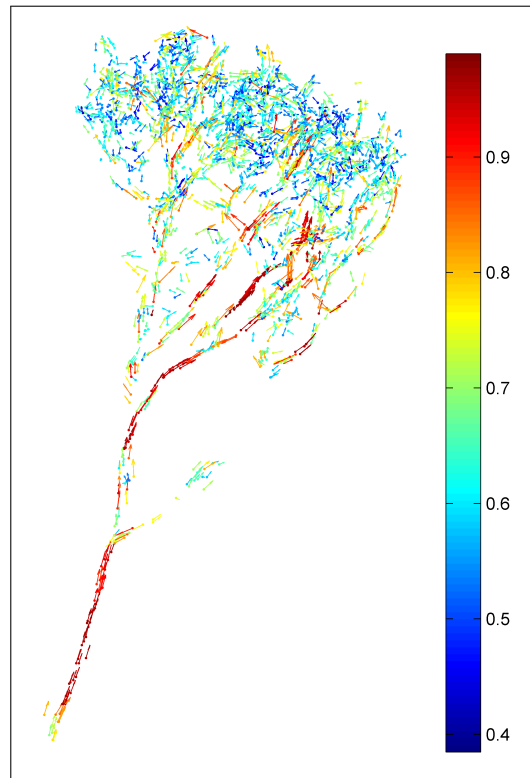


Figure 3.9: A tree coloured by normalized largest eigenvalue at each point. The arrows depict the directions of the corresponding eigenvectors.

For future research it is suggested to classify trees by using the geometric shape of the clusters and a principal component analysis on the neighbourhood of each point to identify trunks. A comparable approach has been presented by [Bremer et al. \(2013\)](#) previously. At each point the three eigenvalues and eigenvectors are calculated using a principal component analysis on the coordinates of the point in question and its k nearest neighbours. Due to the elongated and cylindrical shape of trunks the points on a trunk are characterized by a large first eigenvalue compared to the other two eigenvalues. Further it is assumed that for trunk points the largest eigenvalue corresponds to an eigenvector that points in vertical direction. The three eigenvalues of points in tree crowns on the other hand have mainly similar values. As can be seen in [Figure 3.9](#), a cluster can be classified as a tree if the lower part of that cluster consists of points with large first eigenvalue compared to the other two eigenvalues and if the eigenvector corresponding to the first eigenvalue points in vertical direction. The upper part of the cluster contains points with a relatively small first eigenvalue that is similar to the other two eigenvalues. The principal component analysis based classification is however not implemented and in addition would require much computational power.

3.5 Data Management and Processing

The large amount of data from an ALS project requires that the collected data set is split into tiles to create small files, which can be loaded into the main memory and be then processed. These tiles are usually square areas in the horizontal plane. Due to this splitting, edge effects are created at the edges of each tile. In this particular case this means that for a point near an edge its nearest neighbours might not be detected if these are actually in the neighbouring tile. In addition, a tree on a tile edge is split such that parts of it are contained in more than one file.

To avoid edge effects overlapping tiles are created. This means that for each tile a buffer is created at its edge by adding a small area of the neighbouring tiles as shown by the grey areas in Figure 3.10a such that the grey area of the neighbouring tile is also considered during processing of the degree of change. For further research it is proposed to also use this approach to extract trees, which are at the edge of a tile and are therefore split between two tiles. This could be done as shown by the example in Figure 3.10b, where two trees are on the red edge between tile 1 and 2. Due to the buffer they can be fully extracted. The consequence is that each tree is detected twice, once in tile 1 and once in tile 2. To avoid such duplicates only trees with a particular point, e.g. the highest point, inside a tile should be saved for that particular tile.

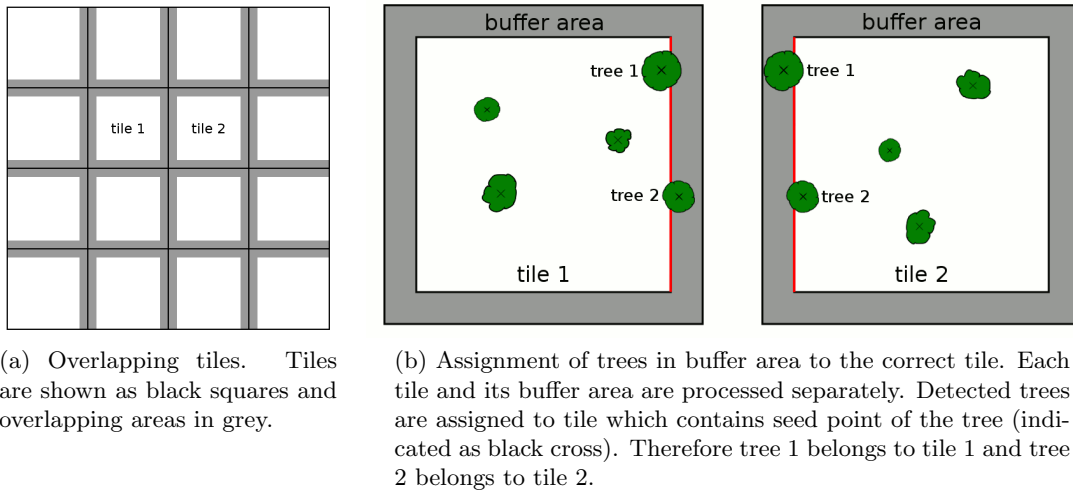


Figure 3.10: Management of tiles over a large area.

Data, Implementation and Results

This chapter includes the description of the test site and the data sets in Section 4.1 and an evaluation of the data quality in Section 4.2. In Section 4.3 the technical implementation of the method is shortly outlined. In the remainder of this chapter the results are presented. This starts with a sensitivity analysis of the degree of change in Section 4.4. The main result of this report, the detection of trees in the sample area, is presented in Section 4.5. Next, the computational performance of the method is evaluated in Section 4.6. Section 4.7 compares the results of different periods and Section 4.8 compares the results to the results obtained from differenced digital surface models. At the end of the chapter the method results are validated.

4.1 Test Site and Data Description

The study area is the Kralingse Bos, a forested area of about 1 km² in size and located in Rotterdam in the Netherlands, see Figure 4.1. The area is flat with elevations ranging from 3 metres below to 1 metre above mean sea level. The trees are mainly deciduous containing several species including poplar, willow, oak, European beech, maple, European hornbeam and European ash. The forest is characterized by multiple layers of canopy and trees of different ages. Tree heights range from approximately 15 to 40 meter as indicated in the Digital Surface Model (DSM) in Figure 4.2. The area is a sustainably managed, recreational and urban forest. Planting of trees in the forest began in 1927 in the eastern part of the park. Meanwhile the management of the forest has changed from a more traditional approach, which included removal of coarse dead wood and dying trees and branches, to the current more sustainable approach. Decaying fallen trees and branches are left on the ground, giving substrates for insects, bacteria, fungi and mosses, and thereby helping to maintain biodiversity.

For the study three ALS data sets were made available by the municipality of Rotterdam. The first data was acquired in November 2008 during leaf-on conditions, the second in March 2010 during leaf-off conditions and the third in March and April 2012 during leaf-on



Figure 4.1: Aerial image of Kralingse Bos obtained in 2008. (Source: Municipality of Rotterdam)

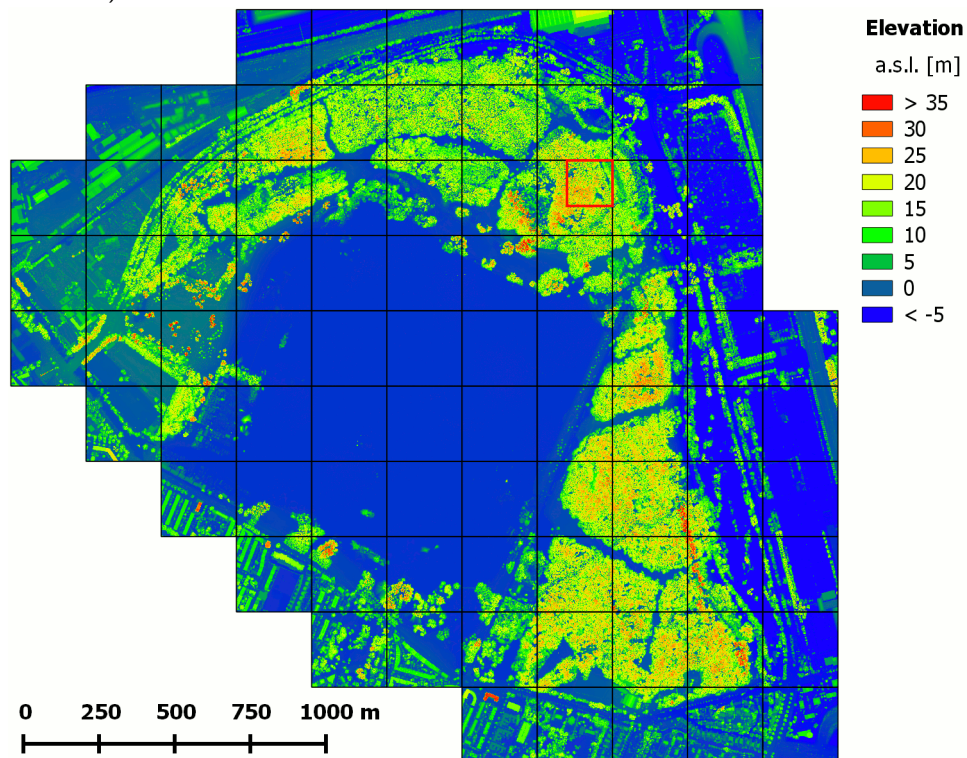


Figure 4.2: Digital surface model of the Kralingse Bos. The model was created with a 1 metre resolution from ALS data acquired in November 2008. The red square indicates the sample research area (see Appendix A).

Table 4.1: Summary of laser scanners, flight parameters and point density within the study area

Parameters	2008 Data Set	2010 Data Set	2012 Data Set
Scanning period	November 2008	March 2010	March/April 2012
Foliation state of tress	Leaf-on	Leaf-off	Leaf-on
Laser scanner	FLI-MAP 400	FLI-MAP 400	Riegl LMS-Q680i
Flight lines	SW-NE / SE-NW	SW-NE / SE-NW	S-N / E-W
Flight altitude (m a.g.l.)	350	350**	450**
Swath width (across track, deg)	± 30	± 30	± 30
Look angles (along track, deg)	+7,0,-7	+7,0,-7	0
Scan frequency (Hz)	150.000	150.000**	400.000**
Laser beam divergence (mrad)	0.45	0.45	≤ 0.5
Pulse density, mean (m^{-2})*	44	42	50
Point density, mean (m^{-2})*	93	64	118
Max. points extracted per pulse	4	2	5

* calculated on 10 m x 10 m grid cells in forested area

** according to flight plan

conditions. For the 2008 and 2010 data the FLI-MAP 400 system was used. The system has three laser look angles in the flight direction, one 7° forward, one nadir and one 7° aftward. In addition to the South-West to North-East flight strips also perpendicular strips in South-East to North-West direction have been acquired to reduce shadows. For the 2012 data the Riegl LMS-Q680i scanner was used, which uses full-waveforms, that are subsequently discretized. During the 2012 project flight strips in North-South and additionally East-West directions were acquired. More information on the laser scanners, flight parameters and point densities is summarized in Table 4.1.

4.2 Data Quality and Co-registration

The quality of the laser scanning data has been evaluated by the Municipality of Rotterdam. For each project the absolute accuracy has been determined at three locations in Rotterdam, which satisfy a set of requirements. These requirements include flatness of the surface, asphalt pavement, and the absence of objects that might influence the GPS or laser measurements. At multiple points at each location the elevation values of GPS measurements have been taken and compared to the elevation values of the laser scanning data. A summary of these absolute accuracies in elevation is provided in Table 4.2. All values of the means, maxima and standard deviations of the measurements are within a few centimetres. The data sets are therefore considered to be of very high quality.

Comparison of two spatial data sets requires their co-registration. Therefore digital terrain models (DTMs) were created for each year separately and subsequently compared. First, in each tile the ground points were extracted with the lasground function in LAStools. The settings for this process were adjusted for good performance in forest environments (using settings wilderness and extra fine), but resulted in the adverse effect of including buildings in the set of ground points. While this deficiency could be corrected with additional processing steps it was decided against it. This is justified by the fact that the residential area around the Kralingse Bos does not belong to the area of research. Next,

Table 4.2: Validation of Z-coordinates performed by the Municipality of Rotterdam at three locations distributed over Rotterdam. The table shows the maximum, the mean and the standard deviation of the differences between a number of GPS measurements at each location and the Z-values of the closest LiDAR point.

(a) 2008 data.				(b) 2010 data.			
	Loc. 1	Loc. 2	Loc. 3		Loc. 1	Loc. 2	Loc. 3
MAX	0.06m	0.05m	0.06m	MAX	0.07m	0.07m	0.08m
MEAN	0.03m	0.01m	0.01m	MEAN	n/a	n/a	n/a
STDEV	0.03m	0.02m	0.02m	STDEV	0.02m	0.03m	0.03m

(c) 2012 data.			
	Loc. 1	Loc. 2	Loc. 3
MAX	-0.055m	-0.028m	0.033m
MEAN	-0.015m	0.002m	0.018m
STDEV	0.012m	0.013m	0.007m

Table 4.3: Quality of vertical co-registration based on the difference in elevation between different years. Only grid cells of the digital terrain models corresponding to paths and roads as shown in Figure 4.3 were considered for the calculation.

	2008/2010	2008/2012	2010/2012
MEAN	-0.004m	-0.011m	-0.008m
STDEV	0.038m	0.033m	0.030m

digital terrain models were created from the extracted ground points using LAStools' las2dem function with a grid cell size of 25 cm. The resulting digital terrain model tiles were merged with gdal.merge from the Geospatial Data Abstraction Library (GDAL). In order to minimize the influence of actual terrain changes (e.g. elevation changes due to leaves, root pits created by fallen trees, water level of the Kralingse Plas, etc.) on the co-registration process only cells belong to terrain, which most likely did not change, should be considered. Further the generation of a digital terrain model should not be influenced by surface morphology and canopy structure. Therefore grid cells corresponding to roads and paths, which satisfy these requirements to a large extent, were extracted from the digital terrain models using topographical vector data from TOP10NL (2011) data. Only these grid cell were used for co-registration. The digital terrain model constructed from the 2008 data can be seen in Figure 4.3 together with the difference of the 2008 and 2012 digital terrain model. The differences between all digital terrain models are summarized in Table 4.3. Here, values that are more than 1.5 times the interquartile range below the first quartile or above the third quartile were considered outliers. The mean values are in the order of 1 cm and the standard deviations in the order of 3 to 4 cm. These results agree with the quality assessment presented above. The co-registration was therefore not refined.

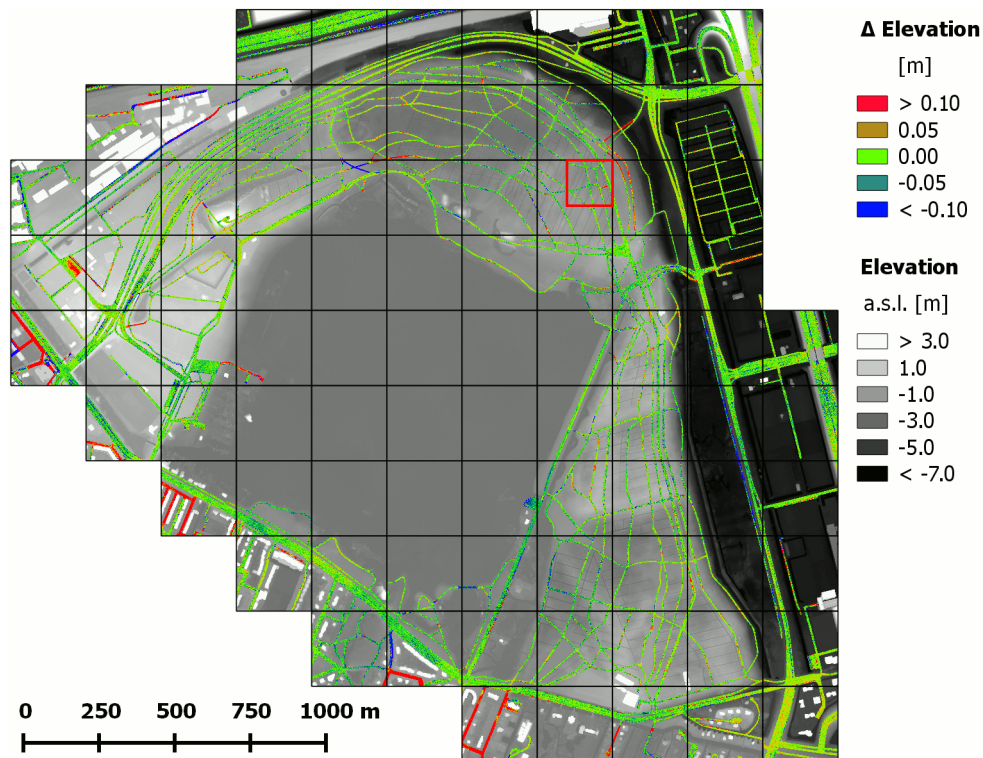


Figure 4.3: Difference in elevation between 2008 and 2012 on paths and roads in the study area. Red indicates a higher elevation in 2012 and blue a lower elevation. In the background the digital terrain model of 2008 is shown in greyscale colours. The red square indicates the sample research area (see Appendix A).

4.3 Implementation

The methodology to extract harvested trees from bi-temporal data of the same area, as presented in Sections 3.1 to 3.4, was implemented using both existing software and self-developed code. For the analysis a small forest patch of 150 times 150 meters was used, containing 2,701,729 points in the year 2008, 1,562,042 points in 2010 and 3,121,007 points in 2012. This study area is indicated by red squares in Figures 4.2 and 4.3 and the corresponding point clouds are given in Appendix A. In addition, a buffer-area of five meters is always added to the reference cloud in order to avoid that the tile boundaries affect the computation of the degree of change. Further, as a pre-processing step ground points were identified using lastools (see Section 4.2) and saved in the compressed .laz format. Only the non-ground points are considered in the compared cloud. All other processing was done in the MATLAB 64-bit (R2014a) environment (MATLAB, 2014). For data input the Matlas tools Toolbox, developed by the Finnish Geodetic Institute (FGI), is used to read the .laz files into the Matlab environment (Puttonen and Litkey, 2014). The function makes use of MATLAB's MEX-functions in order to make the C++ coded readlas function (lastools) callable from MATLAB.

The k nearest neighbours are found using MATLAB's function knnsearch, using again a MEX-function for improved speed and following the algorithm by Friedman et al. (1977)

explained in Section 2.4. For this a kd -tree is built for the reference cloud only. Subsequently, for each non-ground point in the compared cloud and the reference cloud the nearest neighbours in the kd -tree are detected and the resulting distances and indices are stored in separate arrays for the computation of the the degree of change. The computation of the degree of change is vectorized, thus avoiding loops, and optimized for computational speed. While this process is fast, it can temporarily require more memory than is available on normal computers if a large number of points and nearest neighbours is used. After the calculation of the degree of change only non-ground points in the compared cloud, that are classified as changed points, are considered further. For them their nearest neighbours are found for further processing, i.e. for region growing, clustering and classification. Most of these steps were implemented using loops, therefore reducing the performance in MATLAB.

4.4 Sensitivity Analysis of Degree of Change

In order to analyse how the degree of change reacts to variations in point densities and to different values of k a sensitivity analysis is performed. To take into account that the results might be influenced by the chosen pair of data sets, in particular by the foliation states in the data, all possible combinations are evaluated. First the results for the comparison of the 2008 data to the 2012 data in the sample area are analysed, then 2008 to 2010 and finally 2010 to 2012.

4.4.1 Degree of Change from 2008 to 2012

In Section 3.2 it was argued that the degree of change is robust to changes in density. This means that a similar value should be returned independent of the point density in the reference cloud (in this case the 2012 data). To test this hypothesis a simulation is done by varying the point density in the reference cloud by a number of different factors. The simulation is then implemented by calculating the degree of change to the reference cloud once with full point density and once with a reduced point density. This is then repeated with a different factor of point density reduction. For the two results a linear regression model is created, that shows the offset a and slope b as given by Equation 4.1. In the perfect case of point density independence the offset should be equal to zero, the slope equal to one and the goodness-of-fit R^2 equal to one.

$$y = a + b * x \tag{4.1}$$

Figure 4.4 shows the degree of change computed for 10% point density plotted against 100% point density in the reference cloud. The plots show that for k equal to 5 and equal to 25 an offset with a few centimetres and a slope close to one can be achieved. The R^2 values of 0.7 and 0.67 for k equal to 5 and 25 respectively indicate a moderate but significant fit to the hypothesis of density independence considering the tenfold reduction in point density. An tenfold increase in point density can be obtained taking the inverse of the fitted function, resulting in slopes above one. Figure 4.5 shows the degree of change computed for a smaller difference in point density. Here 50% point density and 100%

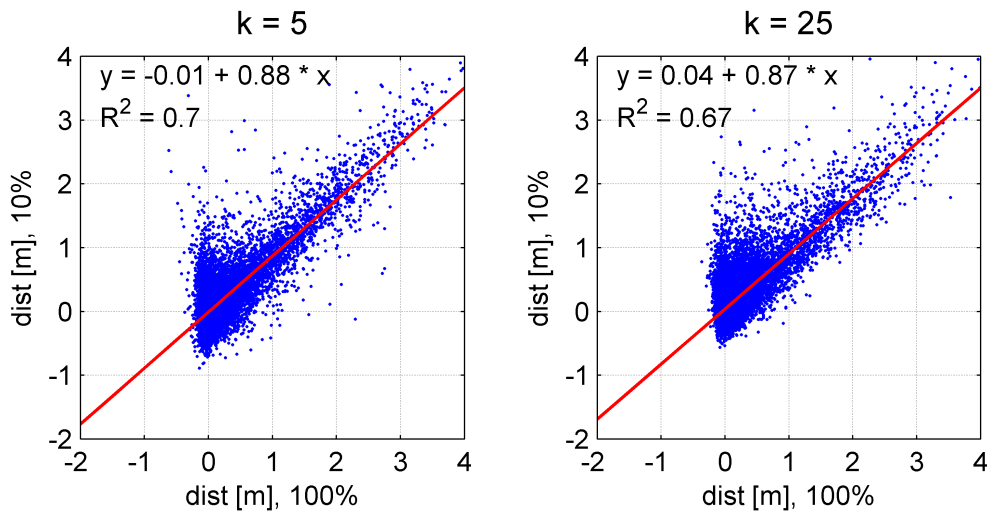


Figure 4.4: Statistical relationship for comparison of 2008 data to 2012 data. Degree of change resulting for full point cloud data (100%) is compared against degree of change for 10% of the data in the reference cloud. Results are shown for $k = 5$ and $k = 25$.

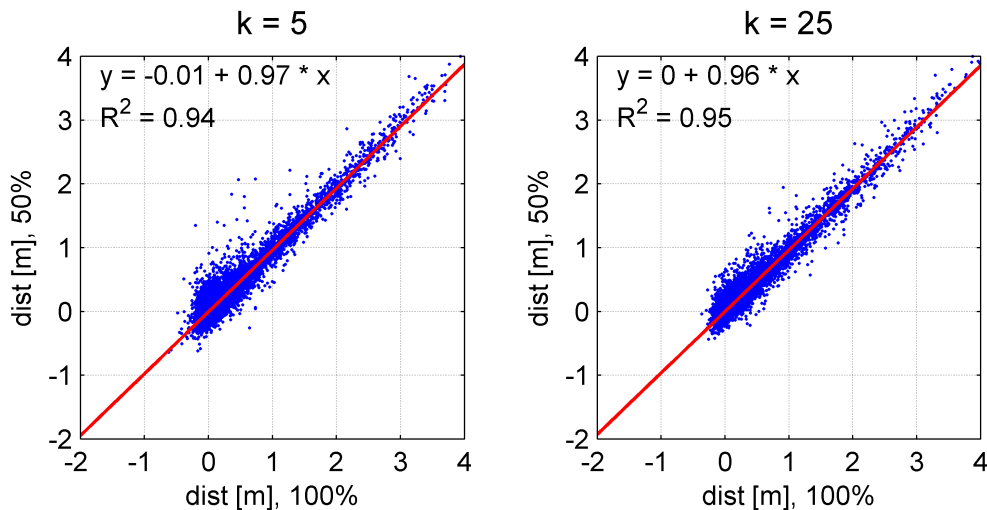


Figure 4.5: Statistical relationship for comparison of 2008 data to 2012 data. Degree of change resulting for full point cloud data (100%) is compared against degree of change for half of the data (50%) in the reference cloud. Results are shown for $k = 5$ and $k = 25$.

point density are evaluated. With offsets within one centimeter, a slope within 4% from one and R^2 values of 0.94 and 0.95 for k equal to 5 and 25 respectively the results for twofold reduction in point density show a much better similarity to the optimal model.

The results obtained after performing the same analysis for various values of k and factors of point density change are summarized in Figure 4.7. For all three measures of the model, i.e. the slope b , the offset a and the goodness-of-fit R^2 , it can be observed that they are closer to the optimal results, i.e. slope b of one, offset a of zero and goodness-of-fit R^2 of one, if the difference in point density is smaller. This is to be expected due to the greater

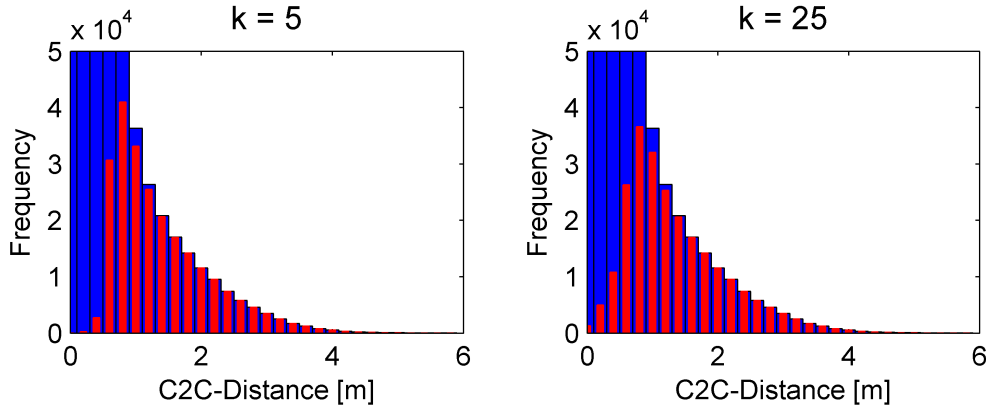


Figure 4.6: Histogram showing effect of degree of change based classification on the basic cloud-to-cloud distance for comparison of 2008 data to 2012 data. Blue bars show the histogram of the basic cloud-to-cloud distance. Red bars show the relative amount that was classified as change using the degree of change with $k = 5$ and $k = 25$.

similarity of the compared data. The resulting slopes show that the degree of change is always smaller for low point densities compared to high point densities and, if the inverse is taken, larger for high point densities compared to low point densities. Further, it can be observed that the value for k influences the outcome. Very low values of k , i.e. below 5, and very large values, i.e. above 25, yield in general the lowest similarity to the ideal model. Values between 5 and 25 seem to behave stable, with the values 5 and 10 being on average closest to the ideal model.

To obtain a classification of points into a changed class or not changed class the threshold given by Equation 3.4 is used. An overview of values of this threshold obtained for different k and five different point densities in the reference cloud is given in Figure 4.8. It can be seen that between 5 and 25 nearest neighbours the threshold is stable and relatively constant for a given point density. In this range it is below 0.5 metre for halve to full density. For 25% of the full point density it is approximately 10 centimetres higher and for 10% approximately 20 centimetres higher.

If the basic cloud-to-cloud distance is calculated, then a very small distance does not necessarily have to be a change because the distance to the next closest neighbours could in fact be much larger. Therefore it is analysed which basic cloud-to-cloud distance the points, which are classified as a change by using the degree of change, have. Figure 4.6 shows this for 5 and 25 nearest neighbours on a histogram. The blue bars show the histogram of the basic cloud-to-cloud distance and the red bars show how many of these points were classified as change. Three particular observations can be made from the two plots. First, several points with a very low basic cloud-to-cloud distance, some even close to zero, were identified to be a change. Secondly, this effect is stronger for larger k . And thirdly, several points with basic cloud-to-cloud distances larger than 1 metre were not classified as change. While it cannot be said with certainty that points classified as change are indeed changes, it can be concluded that the idea of the degree of change should work in theory.

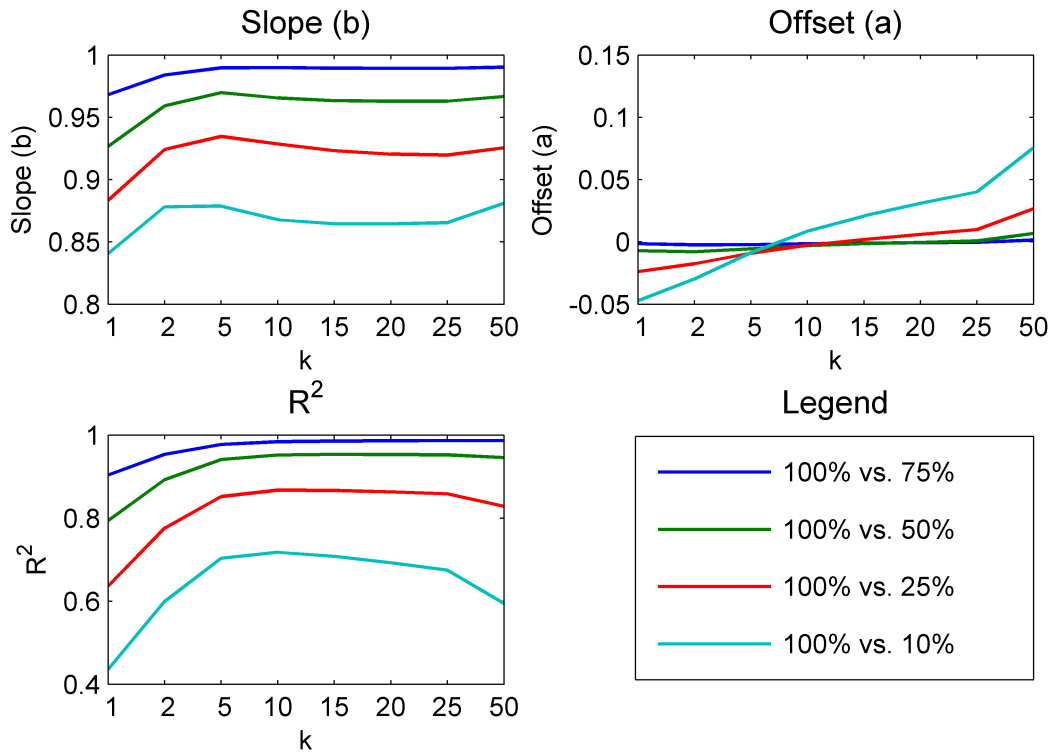


Figure 4.7: Summary of statistical relationships of multiple densities and values of k for comparison of 2008 data to 2012 data.

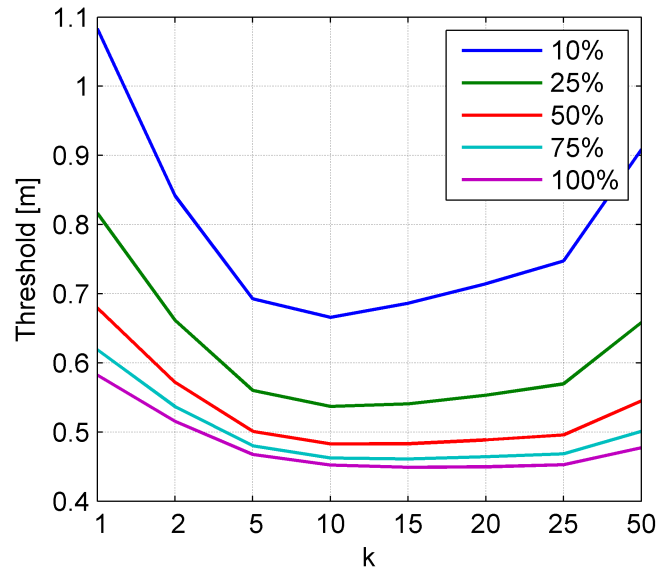


Figure 4.8: Summary of degree of change thresholds for the comparison of 2008 data to 2012 data using different values of k and densities in the reference cloud.

4.4.2 Degree of Change from 2008 to 2010

The data from the year 2010 significantly differs in the foliation state to the data from 2008 and 2012. The former data was acquired during leaf-off condition while the latter two data set were acquired during leaf-on conditions. Therefore it is evaluated separately how the degree of change between 2008 and 2010 reacts to changes in k and point density. However, only the summary of the regression analysis and the summary of threshold values is given.

The results obtained after fitting the linear model for various values of k and factors of point density change are summarized in Figure 4.9. The slope b , offset a and goodness-of-fit R^2 show the same characteristics as in the previous case, but with poorer fitting parameters. The slope b is slightly lower than in the previous comparison, but again the values closest to one are obtained for k equal to 5 or higher. Most of the offsets range between 0 and 5 centimetres. Except for the results for a density of 10%, the smallest offsets are obtained for k equal to 5 or larger. Together with lower R^2 values the summary shows that for the comparison of a data set with leaves to a data set without leaves the degree of change is less independent of point density. This can be explained by the great dissimilarity between data sets that causes a lot of points, in particular points corresponding to foliage, to be distant to the points of the non-foliated tree branches in the reference cloud. Since there is a lot of small change between the two years the interquartile range in Equation 3.4 also increases, thus resulting in high thresholds as can be seen in Figure 4.10. The result is that most of the change in foliation is automatically not classified as change as desired for the detection of harvested trees. The drawback to this is that parts of trees that were harvested might also not be classified as change.

4.4.3 Degree of Change from 2010 to 2012

Also the degree of change for the comparison of the 2010 to the 2012 data is evaluated separately. Again only the summary of the regression analysis and the summary of threshold values are given. In this comparison it has to be considered that the compared cloud has no leaves while the reference cloud is in leaf-on conditions. The results are given in Figure 4.11. The main characteristic are again similar. Here though, the goodness-of-fit R^2 for the model fitting the 10% density data to the 100% density data does not exceed 0.5 for any value of k .

The threshold values obtained are lower than in the previous comparisons. For high densities and k between 5 and 25 the threshold is as low as 0.2 metre and lower. The highest thresholds are obtained for a density in the reference cloud of 10% and are approximately 0.4 meters. This is comparable to the lowest thresholds in Section 4.4.1.

4.4.4 Summary

Summarizing it can be said that the degree of change only conditionally behaves point density independent. While the goodness-of-fit was in most cases intermediate to good, it must be taken into account that significant noise might be present in the degree of change. Nevertheless, the presented model parameters are stable for most values of k .

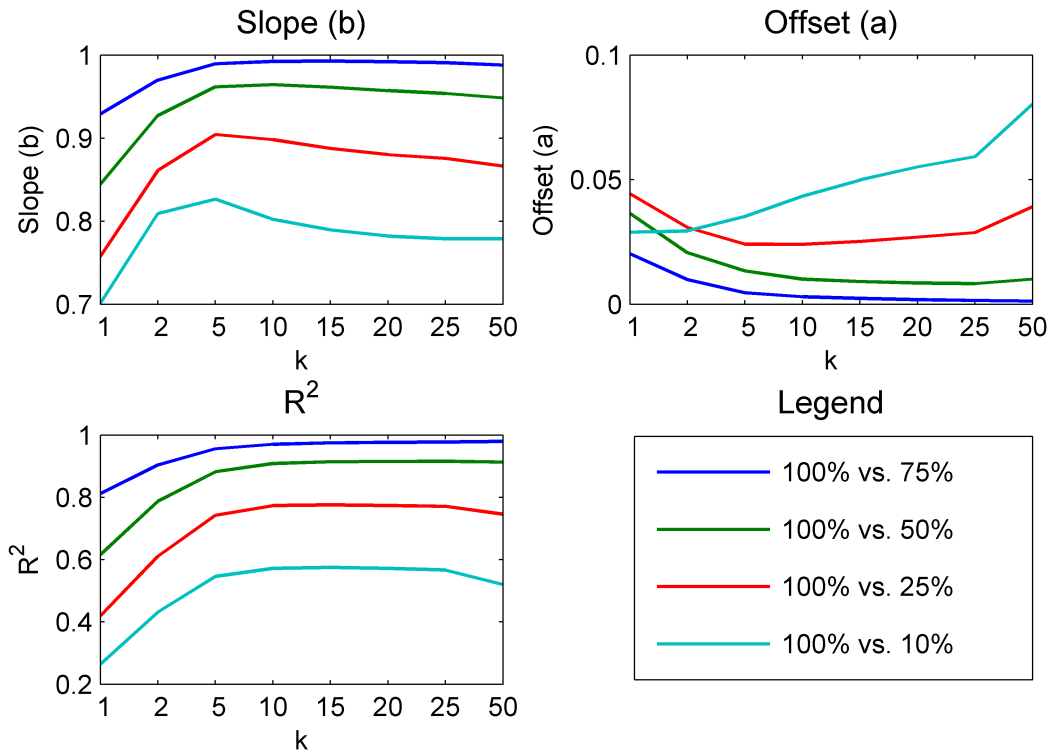


Figure 4.9: Summary of statistical relationships of multiple densities and values of k for comparison of 2008 data to 2010 data.

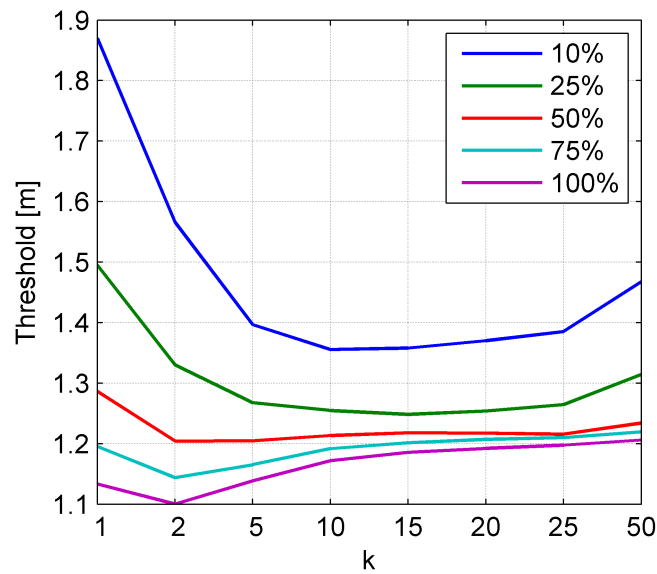


Figure 4.10: Summary of degree of change thresholds for the comparison of 2008 data to 2010 data using different densities and values of k .

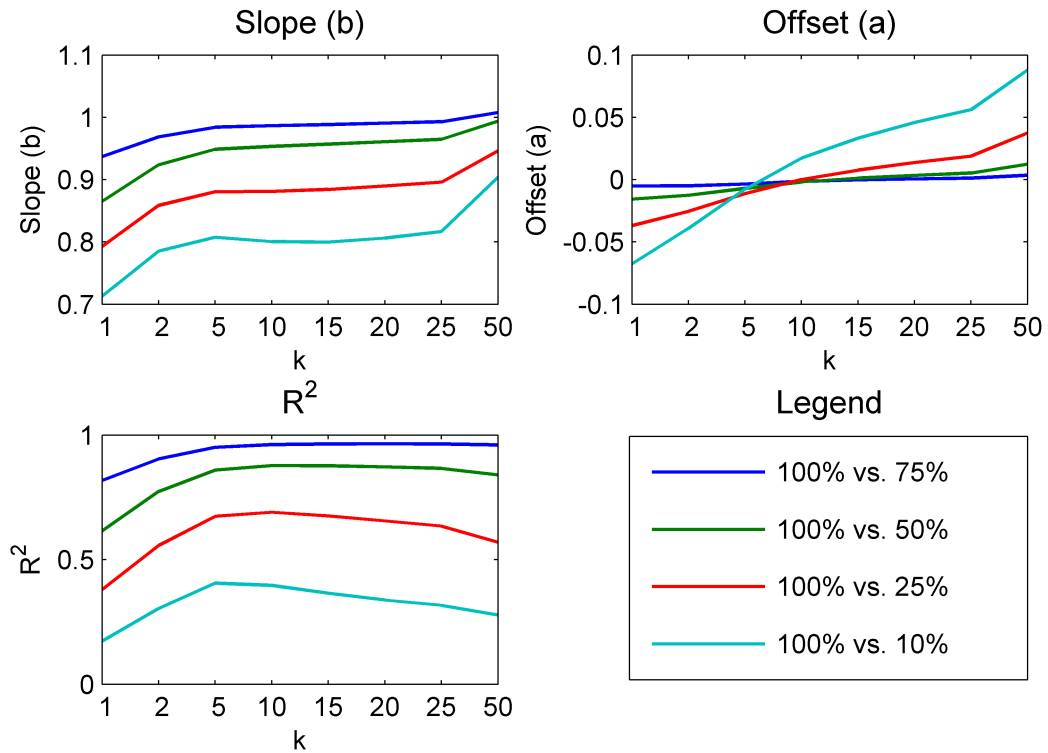


Figure 4.11: Summary of statistical relationships of multiple densities and values of k for comparison of 2010 data to 2012 data.

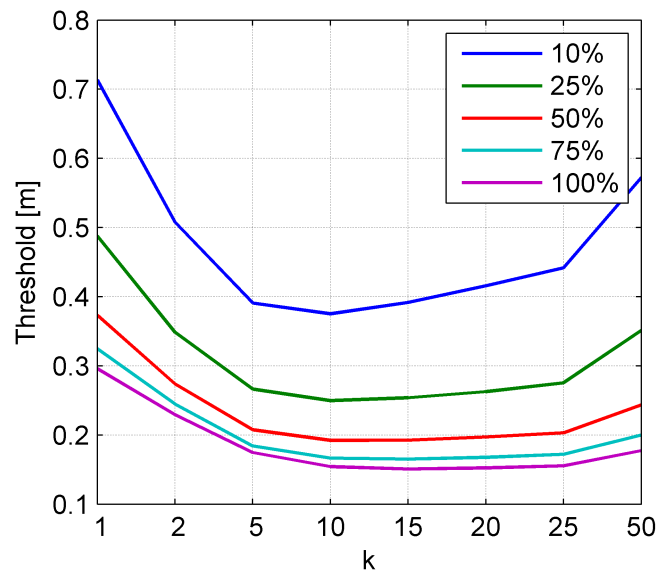


Figure 4.12: Summary of degree of change thresholds for the comparison of 2010 data to 2012 data using different densities and values of k .

On average the best results could be obtained for k equal to 5 and 10. Taking into account that a larger value of k seems to classify more points with a small basic cloud-to-cloud distance as change a value of 10 seems more appropriate (see Figure 4.6). The results are supported by the assumptions that larger values reduce the effect of locality, but on the other hand that smaller values contain less statistical information (Table 3.1).

4.5 Detection of Harvested Trees

The main result of this research is the detection of harvested and fallen trees between the years 2008, 2010 and 2012 in the sample area, which is indicated by the red square in Figures 4.2 and 4.3. All three possible combinations are processed, thus giving the pairs 2008/2012, 2008/2010 and 2010/2012. The corresponding point clouds of each year are shown in Appendix A. To detect these changes the procedure as described in Chapter 3 is applied to the point clouds using full point density. From the compared cloud only non-ground points are used. Finally the results are presented for each comparison.

In the first step of the methodology the points in the compared clouds were identified as change with k set equal to 10 because this is an optimal value according to the sensitivity analysis in Section 4.4. The used thresholds were 0.45 metre for the 2008/2012 comparison, 1.17 metres for the 2008/2010 comparison and 0.15 metre for the 2010/2012 comparison. The discrepancy between these values is explained by the difference in foliage stage as was discussed in Section 4.4. In the second step the points that were identified as change were further clustered into spatially connected segments using the

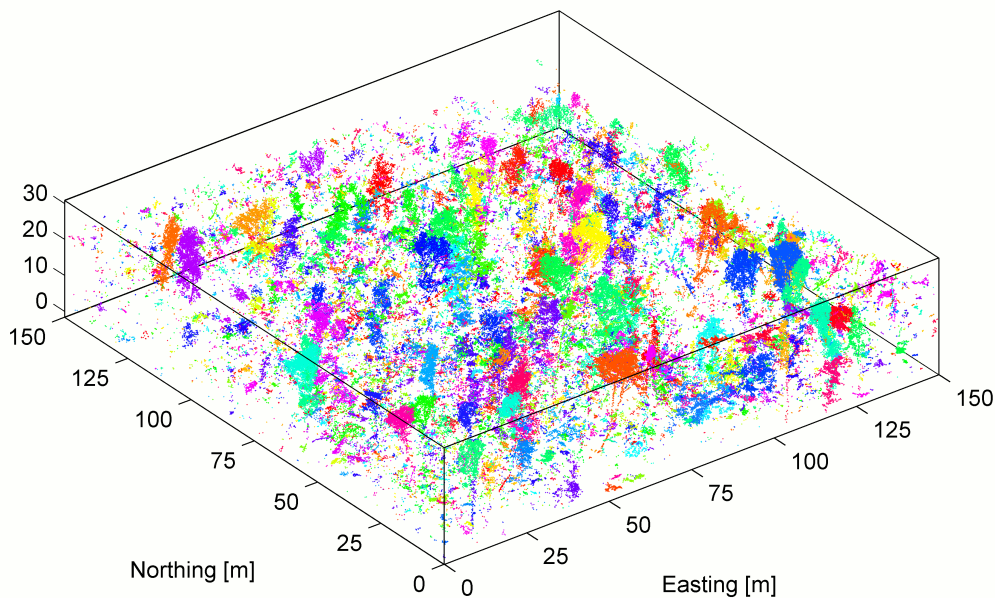


Figure 4.13: Resulting clusters after region growing for the comparison of the 2008 and 2012 data. Each cluster is plotted in a random colour.

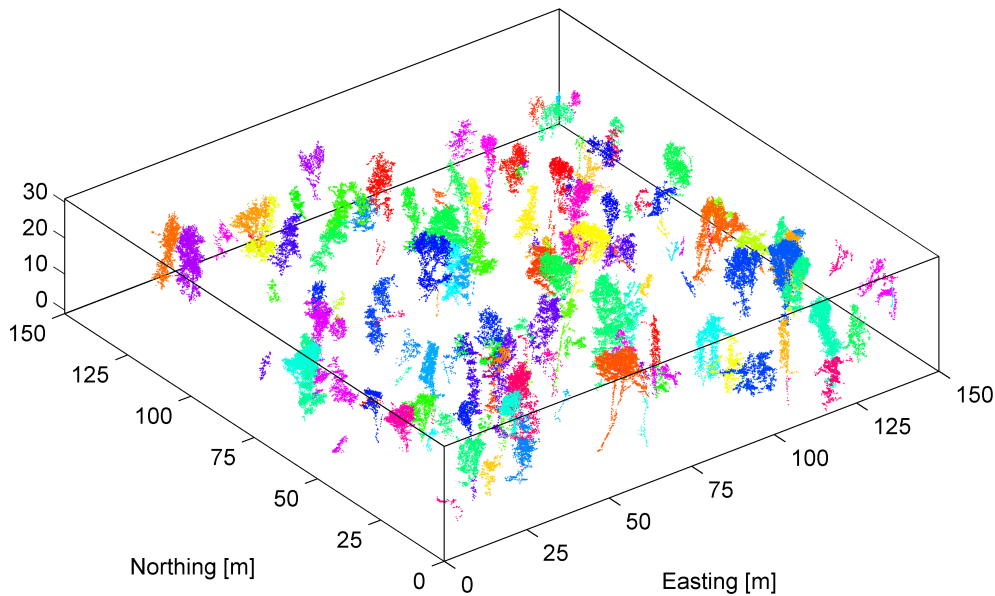


Figure 4.14: Resulting trees after classification for the comparison of the 2008 and 2012 data. All clusters are plotted in the same colour as in Figure 4.13.

described region growing method and then merged into larger objects using the bottom-up clustering approach. During the region growing process the 20 nearest neighbours of the seed points were analysed and a value of one standard deviation was set for the Mahalanobis distance. The bottom-up clustering required a minimum distance between clusters of 1 meter to establish a connectivity of clusters and a maximum of 5 meters was set for the horizontal distance between cluster centroids. An example for the comparison of the 2008 to the 2012 data is shown in Figure 4.13. Clearly many small clusters exist as well as several larger clusters showing trees.

In the third step the resulting clusters were further classified as trees if their height was more than ten meters, the vertical expansion was at least five meters and larger than the horizontal expansion. The classified trees are shown in Figure 4.14 in the same colour as in Figure 4.13. Examples of clusters that are classified as trees and other objects are shown in Figure 4.15 and Figure 4.16, respectively. The tree examples show that for some trees the trunk could either not be identified as change or is missing due to over-segmentation of the tree. Another explanation for a missing trunk could be the scanning process, which might result in missing data points of the trunk. The fourth tree appears to include a branch of a neighbouring tree and is thus slightly under-segmented. The clusters that were not classified as trees include parts of crowns in the first two images, other branches in the third image and undergrowth in the latter two images.

An overview of the number of detected trees is given in Table 4.4. In total there are 150 harvested trees detected between 2008 and 2012, where 49 of these are higher than 25 metres. Between 2008 and 2010 a total of 103 trees was detected and between 2010 and

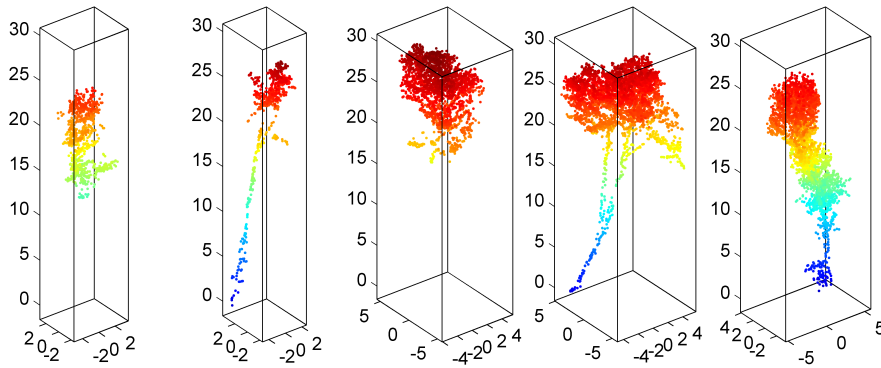


Figure 4.15: Clusters, that are classified as trees.

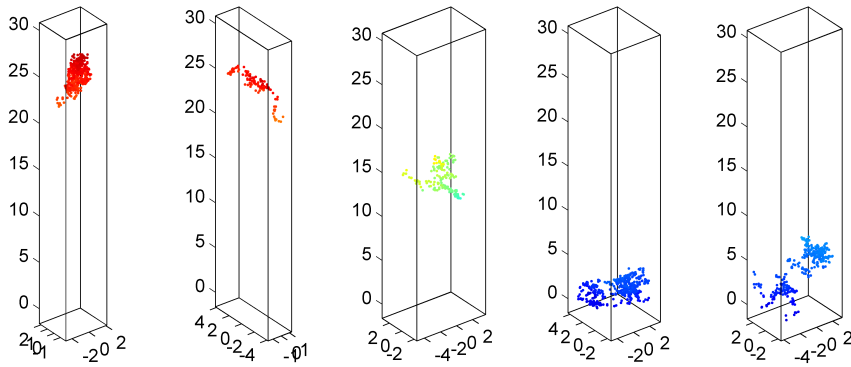


Figure 4.16: Clusters, that are not classified as trees.

2012 a total of 89 trees. Clearly the sum 192 of the latter two, i.e. 2008 to 2010 and 2010 to 2012, does not match the number of 150 trees from 2008 to 2012. The same can be observed for the height groups of 15 to 20 metres and 20 to 25 metres. The numbers for smaller and larger trees match moderately. This discrepancy is evaluated in the following section.

Table 4.4: Number of detected harvested trees per tree height and data pair.

Tree height	2008/2012	2008/2010	2010/2012
$h \leq 15\text{m}$	35	14	19
$15\text{m} < h \leq 20\text{m}$	34	30	20
$20\text{m} < h \leq 25\text{m}$	32	35	28
$25\text{m} < h$	49	24	22
Total	150	103	89

4.6 Computational Performance

An important aspect of this research is the analysis of the computational performance of the developed method. Therefore the mean processing time at each step of the method (see Section 3.1) and their major sub-steps is obtained. The same sample area and the same settings as in Section 4.5 are used for all three possible comparison combinations. Further, in order to get reliable information, at each sub-step the mean processing time of three runs is calculated. The data was processed on an AMD Phenom II X4 955 processor with 3.2Ghz and with 8GB DDR3 installed physical memory (RAM).

The first step calculates the degree of change. Its sub-steps are the creation of a kd -tree for the reference cloud, for each point of the compared cloud finding the k nearest neighbours in this kd -tree and their distances, similarly for each point of the reference cloud finding the k nearest neighbours also in the same kd -tree and their distances, and finally the computation of the degree of change. The second step consists of the region growing process and the merging of the resulting clusters. The third step consists of the classification of the merged clusters.

The resulting processing times are summarized in Table 4.5. The method required the most time, 332.3 seconds, for processing the comparison of the 2008 data to the 2012 data and the least time, 97.4 seconds, for the comparison of the 2010 to 2012 data. The results are well related to the number of points and clusters at each step (see Table 4.6). The most time in step 1 was required for the detection of nearest neighbours, which depended on the number of points in the reference cloud, including a buffer of 5 metres around the tile, and the number of non-ground points in the compared cloud. Once the nearest neighbours and the distances to them were known the degree of change was calculated in approximately one second or less.

In step 2 the time to extract spatially connected objects from the changed points varied significantly between the three different comparisons. This depended on the number of changed points (Table 4.6) during region growing. Most striking however is the observation that the time to merge clusters differed by a factor of 25 between the 2008 to 2012 comparison (156.0 seconds) and the 2010 to 2012 comparison (6.1 seconds) and a factor of 10 between the 2008 to 2010 comparison (60.3 seconds) and the 2010 to 2012 comparison (6.1 seconds). It is assumed that this difference is related to the number of merging instances, i.e. the difference between number of clusters after region growing and the number of clusters after cluster merging. The reason for this assumption is the observation that the number of clusters after region growing is similar for the 2008 to 2010 and the 2010 to 2012 comparisons (15,455 and 15,056 respectively). On the other hand the difference in computation time is in agreement with the difference in the number of merging instances (15,455 minus 4,013 and 15,056 minus 11,967 respectively). Finally, the classification in step 3 was performed in very short time in all three cases.

Summarizing it can be said that the number of points and clusters that have to be processed is progressively reduced at each step. Nevertheless, in several instances this does not lead to a reduction in computation time. In particular the merging of clusters appears to have a high computational complexity, resulting in long computation times if many clusters have to be merged. In the worst case the method allowed to detect harvested or fallen trees in a tile of 150 times 150 metres in 332.3 seconds. Projecting

Table 4.5: Computational performance of the method. The mean processing time for each step and sub-step is shown in seconds.

Steps	Sub-steps	2008/2012	2008/2010	2010/2012
Step 1	Building <i>kd</i> -tree of ref. cloud	15.0	7.3	15.1
	<i>k</i> NN from comp. to ref. cloud	28.3	26.4	11.7
	<i>k</i> NN in ref. cloud	41.1	19.8	41.4
	Calculating degree of change	1.1	1.0	0.5
Total of step 1		85.5	54.5	68.7
Step 2	Region growing	89.6	65.7	21.1
	Cluster merging	156.0	60.3	6.1
	Total of step 2	245.6	126.0	27.2
Step 3	Classification	1.2	0.5	1.5
Total		332.3	181.0	97.4

Table 4.6: Number of points and clusters at different stages of the change detection process.

Stage/item	2008/2012	2008/2010	2010/2012
All points in ref. cloud (incl. buffer)	3,543,833	1,766,380	3,543,833
All points in comp. cloud	2,701,729	2,701,729	1,562,042
Non-ground points in comp. cloud	2,086,596	2,086,596	878,819
Changed points in comp. cloud	239,593	173,737	74,291
Clusters after region growing	25,755	15,455	15,056
Clusters after cluster merging	9,075	4,013	11,967

this time to an area of one square-kilometre in size the method would require 4 hours and 6 minutes and therefore can be considered to be still feasible for forestry management or other applications. For the best case of 97.4 seconds this would project to 1 hour and 12 minutes. However, non-linear increase in computation time has to be expected if the size of the processed tiles is increased.

4.7 Comparison of Results

The detected trees of the three different data pairs from Section 4.5 are compared in this Section in order to analyse their agreement. Theoretically, all trees that are detected in the comparison of the 2008 and 2010 data must be also detected in the comparison of the 2008 and 2012 data. Further all trees detected between 2010 and 2012 should be also detected between 2008 and 2012. Vice versa all trees detected between 2008 and 2012 must be either detected between 2008 and 2010 or between 2010 and 2012. In case of disagreement it must be the case that either a disappeared tree was not detected in one of the comparisons, i.e. an omission error, or an object was wrongly classified as disappeared tree, i.e. an commission error.

Figure 4.17 shows all detected harvested trees between 2008 and 2010 in blue and the trees harvested between 2010 and 2012 in green. Their positions, calculated as the horizontal centre of the highest fifty percent of points corresponding to a tree, are marked by crosses. For each of these trees the best matching tree, that was detected between 2008 and 2012,

was identified. Best matching means the closest tree that is not further than two metres away and that was not matched to another closer tree already. Trees that had a match to a tree harvested between 2008 and 2012 are marked with red crosses and non-matched trees are marked with black crosses. Similarly, Figure 4.18 shows all detected harvested trees between 2008 and 2012 in red and their positions as crosses. Trees that had a match to a tree harvested between 2008 and 2010 have green crosses and trees that had a match to a tree harvested between 2010 and 2012 have blue crosses. Non-matched trees are marked with a black cross. In both images it can be seen that many trees were not matched.

This disagreement between the results can have several reasons. In principle a harvested tree might not be detected correctly by the degree of change and thus is not classified as a harvested tree or its horizontal center is biased. Also the threshold that was used for each comparison differs, which means that more of the edges of a harvested tree are not classified as change the larger the threshold is. More likely is that during the individual tree detection a tree is over- or under-segmented, thus leading to a wrong classification or position. An example of an over-segmented tree in one comparison but not the other is shown in Figure 4.19. In the images all detected changes, including both trees and other objects, are displayed in individual colors and non non-changed points in black. An even more drastic error is seen in Figure 4.20, where the tree from the 2008 to 2012 comparison is under-segmented while in the 2010 to 2012 comparison it is over-segmented. An example, where changes in the lower vegetation were classified as removed trees and could not be matched, is shown in Figure 4.21. Here the change between the 2008 to 2012 comparison and the 2010 to 2012 comparison is affected by the change of foliage between 2010 and 2012, thus leading to slight differences between the detected objects. Similarly, the matching might fail due to difference caused by natural growth and regrowth.

An overview of the results is given in Table 4.7. It can be seen that for each data pair only about half of the detected trees could be matched with trees in another data pair. For small trees the matching rate is even lower and large trees with a height above 25 metres could be matched best. Height in this case means the measured height in the compared cloud. Exceptionally low however is the matching rate for trees detected between 2010 and 2012. Here only 13 out of 22 trees large trees could be matched to trees detected between 2008 and 2012. For the large trees harvested between 2008 and 2010 all trees found a match to trees harvested between 2008 and 2012. Despite of the low agreement for small trees, which can be explained by the presented problems, it can be concluded the method is capable of detecting small, i.e. suppressed, trees.

Table 4.7: Comparison of detected harvested trees matched between different data pairs.

Tree height	2008/2012 trees matched to 2008/2010 + 2010/2012 trees	2008/2010 trees matched to 2008/2012 trees	2010/2012 trees matched to 2008/2012 trees
$h \leq 15\text{m}$	10 out of 35	6 out of 14	5 out of 19
$15\text{m} < h \leq 20\text{m}$	17 out of 34	11 out of 30	6 out of 20
$20\text{m} < h \leq 25\text{m}$	17 out of 32	12 out of 35	9 out of 28
$25\text{m} < h$	42 out of 49	24 out of 24	13 out of 22
Total	86 out of 150	53 out of 103	33 out of 89

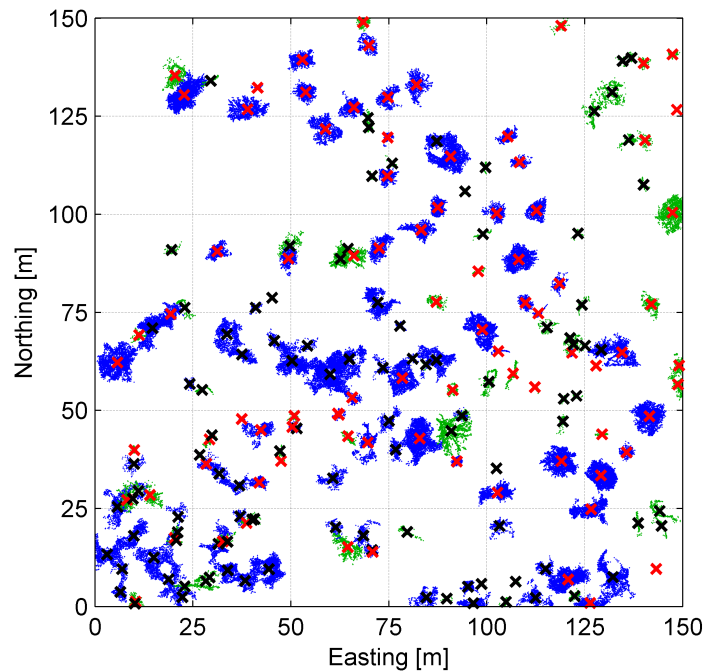


Figure 4.17: Top view of detected trees harvested between 2008 and 2010 in blue and between 2010 and 2012 in green. Their position is indicated by crosses, where a matching to detected trees harvested between 2008 and 2012 is indicated by red crosses and no matching by black crosses.

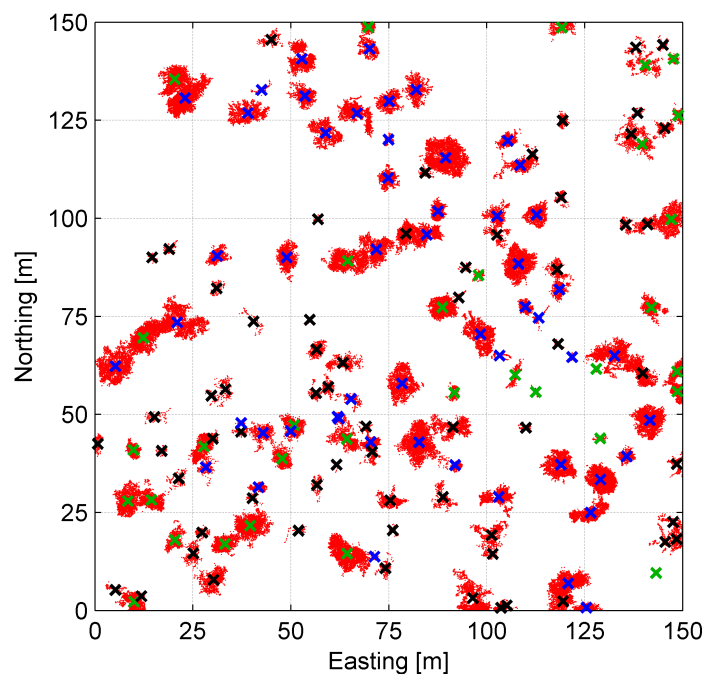


Figure 4.18: Top view of detected trees harvested between 2008 and 2012 in red. Their position is indicated by crosses, where a matching to detected trees harvested between 2008 and 2010 is indicated by blue crosses, between 2010 and 2012 indicated by green crosses and no matching by black crosses.

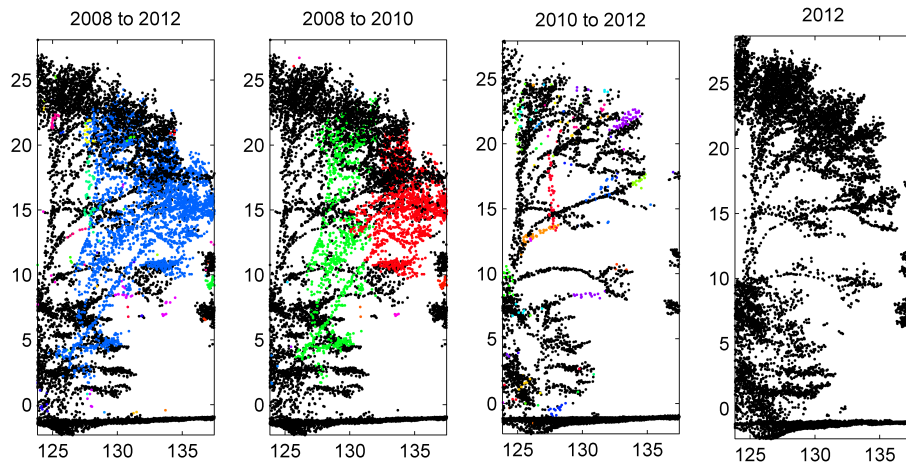


Figure 4.19: Error due to over-segmentation of a harvested tree in one comparison.

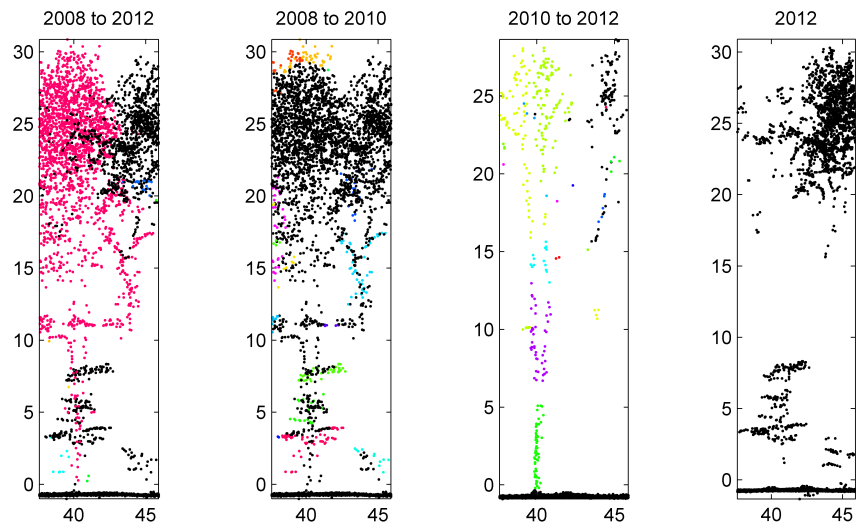


Figure 4.20: Error due to over- and under-segmentation of a harvested tree in different comparisons.

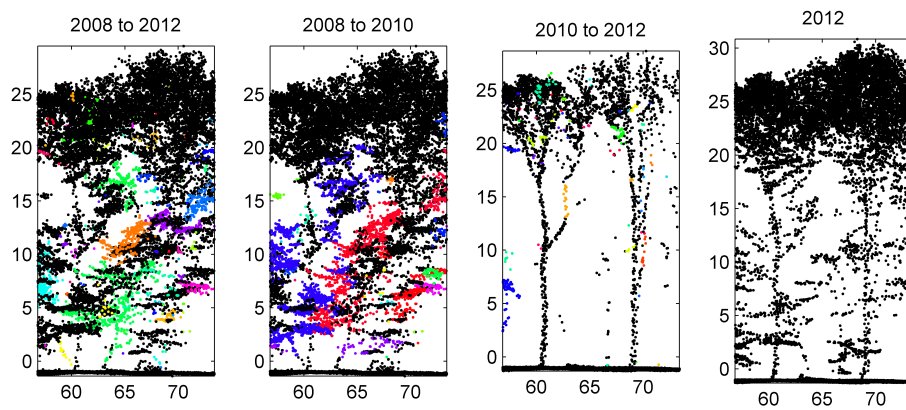


Figure 4.21: Error caused by different foliage states in the reference clouds.

4.8 Comparison to Differenced Digital Surface Models

In Section 1.1 it was addressed that several studies focused on canopy height models to detect changes in forests. To show the potential of the presented method to detect suppressed harvested trees and in general changes below the canopy surface it is compared to the method of differencing digital surface models (or equivalently canopy height models). For each of the years 2008 and 2012 a separate digital surface model is created using a grid with a resolution of 25 centimetres. Each grid cell is filled with the height of the highest point in that grid cell and empty cells are filled by interpolation. Finally the digital surface model of the 2012 data is subtracted from the digital surface model of the 2008 data, such that a reduction in height in a grid cell appears as a negative value and an increase in height as a positive value.

The resulting differenced digital surface model is shown in Figure 4.22. Red shows a reduction in height and therefore could represent a harvested tree and green shows an increase in height and can be linked to either vertical or horizontal growth. The previously detected harvested trees are marked by crosses and their crown size is indicated by circles. Clearly it can be seen that all larger red areas are also marked with a cross and circle. This shows that the developed method is at least as suitable for the detection of dominant trees. Further it can be seen that many of the locations marked with a cross have no reduction in height, meaning that the change must have happened below the canopy surface. Nevertheless, if one compares these suppressed harvested trees with the results in Figure 4.18 one can see that many of these trees did not have a matching tree in another data pair.

4.9 Validation Based on Manual Manipulation

No field work was performed for the study area during the time of the acquisition of the data. Therefore no reference data is available for validation. In order to test the methodology anyhow, fifteen trees were removed from the 2012 data using CloudCompare. First a rough segmentation was performed by cutting out a polygonal area of each tree from the top. Subsequently parts not belonging to the tree were removed. The manually extracted reference trees are shown in Figure 4.23. Additionally a Gaussian noise with a standard deviation of 5 centimetres was added to the x-, y-, and z-coordinates of the points in the manipulated 2012 data. The original 2012 was then compared to the manipulated 2012 data to analyse how many of the removed reference trees can be detected.

Similarly to Section 4.7 a detected tree and a reference tree are matched if the distance between their position is smaller than 2 metres. Other trees, that are not matched, are either omission errors if reference trees were not correctly detected or commission errors if detected trees have no matching reference tree. This information is used to calculate the total accuracy (*Accuracy*) in Equation 4.2, the omission error (*Omission*) in Equation 4.3 and the commission error (*Commission*) in Equation 4.4. Here N_m is the number of matched trees, N_r the number of reference trees and N_d the number of detected trees.

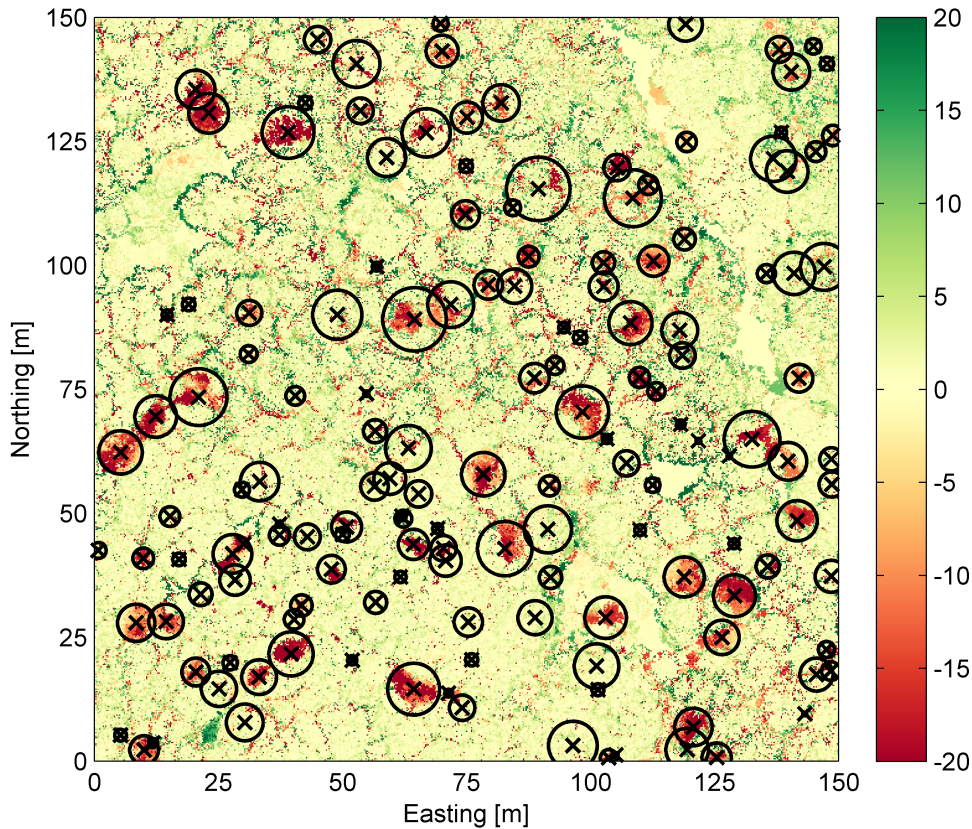


Figure 4.22: Detected harvested trees shown as black circles and laid over the difference between the 2008 and 2012 digital surface models. Red indicates a reduction in elevation and green an increase in elevation over that period.

$$Accuracy = \frac{N_m}{N_r + N_d - N_m} * 100 \quad (4.2)$$

$$Omission = \frac{N_r - N_m}{N_r} * 100 \quad (4.3)$$

$$Commission = \frac{N_d - N_m}{N_d} * 100 \quad (4.4)$$

The validation procedure was performed once with the automatically calculated threshold for the degree of change using Equation 3.4, which result in 0.08 metre, and once with the threshold set to 1.0 metre. Figure 4.24 shows the matching of detected trees and reference trees using the 0.08 metre threshold. All detected trees are plotted in green and their positions are marked with crosses. The positions of the reference trees are marked with circles. The attached numbers give the distances between the positions of matched trees. All fifteen reference trees could be matched to detected trees and in total twenty three trees were detected, thus resulting in eight commissions (Table 4.8). This results

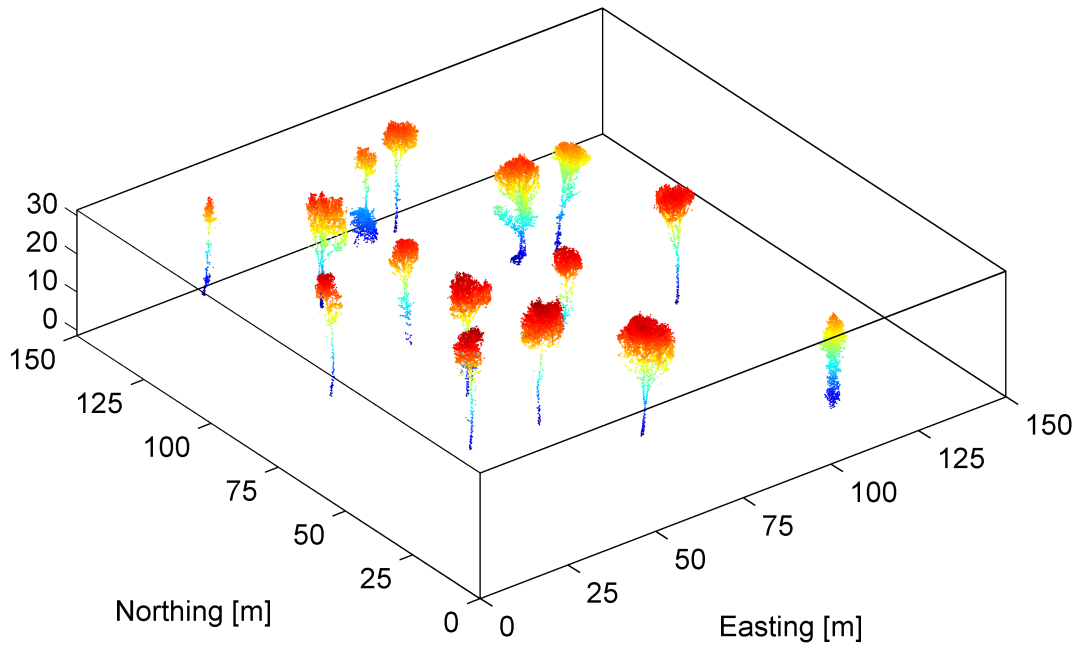


Figure 4.23: Manually extracted trees from 2012 data set.

in an overall accuracy of 65%, and omission error of 0% and an commission error of 35% (Table 4.9). The commission errors are caused by four trees that were over-segmented and four trees that were wrongly identified as removed trees even though no trees were removed at their location. The latter is caused by the added noise, the very low threshold and by the presence of isolated points and very small clusters, which are too far from all other points and therefore have a too large degree of change.

Table 4.8: Summary of validation results for two different thresholds.

Threshold	0.08m	1.0m
Reference trees N_r	15	15
Detected trees N_d	23	16
Omissions	0	0
Commissions	8	1

Table 4.9: Overall accuracy and error rates for two different thresholds.

Threshold	0.08m	1.0m
<i>Accuracy</i>	65%	94%
<i>Omission</i>	0%	0%
<i>Commission</i>	35%	7%

In Figure 4.25 the resulting matches with a threshold of 1.0 metre are shown. Again all fifteen reference trees were detected correctly. Only one commission error is present due to over-segmentation of a tree. An overall accuracy of 94% was achieved in this case. The omission and commission errors are at 0% and 7% respectively (Table 4.9). In this case smaller parts, like trunks, of potentially over-segmented trees are not present due to the higher threshold. It can be further seen that the correctly detected trees are smaller in size, i.e. the green area is smaller. A larger threshold therefore means that the edges of the detected trees and trunks are likely to be disregarded. As a result of this the estimated position of these trees is less accurate as can be seen by the larger distances in Figure 4.25 compared to Figure 4.24. This effect could potentially lead to difficulties in matching detected and reference trees in some cases.

The results show that the method works well to detect large removed trees. Nevertheless, the method results in a large amount of false positives, which is strongly influenced by the threshold, the clustering and as a consequence of these also by the classification. Small trees, especially suppressed trees, were not validated due to the difficulty to extract these manually from the data. Also other environments, for example higher tree densities, were not validated.

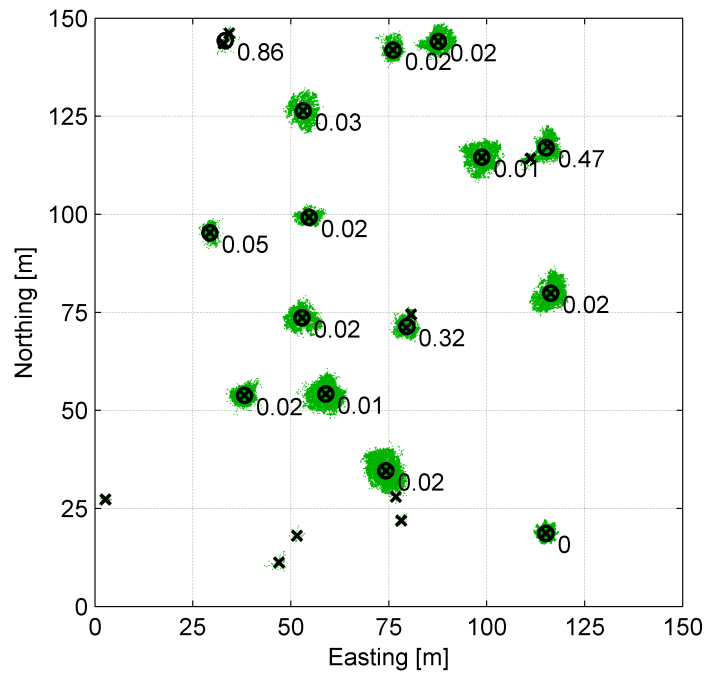


Figure 4.24: Validation for detection of manually harvested trees using a threshold of 0.08 metre. Trees detected by the method are shown in green. Crosses indicate the position of the detected trees and circles the manually removed reference trees. Next to them their horizontal distance is shown in metres.

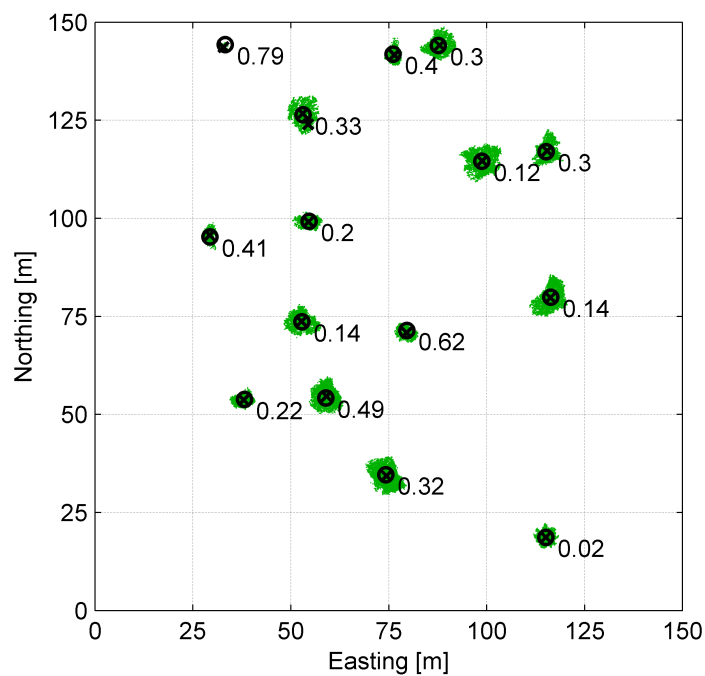


Figure 4.25: Validation for detection of manually harvested trees using a threshold of 1.0 metre. Trees detected by the method are shown in green. Crosses indicate the position of the detected trees and circles the manually removed reference trees. Next to them their horizontal distance is shown in metres.

Conclusions and Recommendations

In this final chapter first the research is reviewed based on the problem statement and research questions in Chapter 1. At the end an outlook towards further development of the methodology and additional applications of it is given.

5.1 Conclusions

The main objective of this thesis was to develop a methodology that identifies changes in forests using multi-temporal high density ALS data. In particular the focus was on the detection of harvested and fallen trees, while smaller changes should be identifiable as well. Substantial importance was given to the exploitation of the full three-dimensional information available in the raw point cloud and to computational performance. The main objectives of this thesis can be identified by the four sub-questions that are coupled to the main research question. In the following, the findings to each sub-question are elaborated and followed by the findings to the main research question.

1. *How can differences between multi-temporal ALS data be detected in the three-dimensional space?*

In Section 3.2 an adapted cloud-to-cloud comparison approach that identifies differences between multi-temporal ALS data was presented. The developed approach directly compares raw bi-temporal data and works on the basis of each individual point in the compared point cloud. It therefore works inherently in the three-dimensional space. The difference at a query point in the compared cloud is realized by the determined degree of change, a value that is based on the mean of the distances to query point's nearest neighbours in the reference point cloud. In addition, effects due variations in point density in the reference cloud are reduced by integration of the spread between points of the reference cloud into the cloud-to-cloud comparison. This effect was confirmed by studying the sensitivity of the degree of change to variations in point density in Section 4.4.

In view of alternative methods, which have been applied in forests, the point based approach proves that small and local differences in between the terrain and the canopy surface can be detected under the given circumstances of high density data. This was visible throughout examples of identified changed objects (Sections 4.5, 4.7 and 4.8). So far, other methods applied in forestry either disregard the space between terrain and canopy surface or disregard locality by analysing the vertical point distribution over large grid cells. Further, the degree of change has been used as an indicator for change only and does not represent an explicit magnitude of change.

2. *How can harvested and fallen trees in forests be extracted from differences detected between multi-temporal ALS data?*

In order to detect harvested and fallen trees only points with a degree of change above a certain threshold are considered. This threshold adapts to differences in foliation stages in order to identify only large changes, like harvested or fallen trees. The disadvantages of the threshold are falsely identified changes if it is low and the exclusion of actually changed points if it is large (Section 4.9). Next, points identified as change are clustered into spatially connected regions (Section 3.3). First region growing is applied to merge spatially close points into clusters. Secondly, an object oriented bottom-up approach is used to merge the clusters using the connectivity of clusters and the horizontal distance between clusters as parameters to identify which clusters are most suitable for merging. The resulting clusters are then classified as trees if they meet requirements on the cluster shape (Section 3.4).

Due to the two step clustering approach the shape of trees is considered and yet partial trees, crowns and stems, other small objects or their parts and isolated point can be identified as separate clusters (Sections 4.5 and 4.7). The tree extraction approach works in the three-dimensional space and it is assumed that an individual tree detection method that works on two-dimensional grids would fail in the situation of processing a few trees and a large number of small tree parts. Despite of its three-dimensional nature and the object oriented approach, the extraction however also suffers from both under-segmented and over-segmented of trees. These errors are in particular influenced by the defined parameters for the clustering procedure.

3. *What is the computational performance to extract these changes?*

The computational performance of the whole procedure is evaluated in Section 4.6. By projecting the obtained computation time to an area of one square-kilometre in size it can be estimated that the method would require approximately 4 hours in the worst case and only 1 hour and 12 minutes in the best case, thus making it feasible for real applications. During the whole procedure the amount of data is reduced starting from all points, then to non-ground points, to changed points, then to small cluster and to merged clusters and finally to trees. The large number of points at the first step can be efficiently handled using a *kd*-tree (Section 4.3). At the second step it was shown that despite of the reduction in the number of points the required processing time cannot be kept short consistently. In particular the merging of clusters has shown to be a potential bottleneck in the procedure. The reason for this is the necessity to update the relationships between clusters each time two clusters are merged into a new one. Since only the relationships between connected

clusters are considered this implementation is nonetheless assumed to be faster than other bottom-up clustering approaches that usually require large similarity matrices containing similarity information between all clusters (e.g. agglomerative clustering). Additionally, it must be assumed that without a reduction of data, i.e. working with individual points, the bottom-up clustering would be computationally infeasible for standard computers.

4. *How can the detected changes be validated?*

For this research no reference data was available for validation. As a consequence fifteen dominant trees were manually removed from a data set in order to test if these reference trees could be identified by the method (Section 4.9). An overall accuracy of 65% with an omission error rate of 0% and a commission error rate of 35% was achieved with the developed method. By increasing the threshold of the degree of change to 1 metre the overall accuracy could be increased to 94%. The perfect omission rate agrees with findings from the qualitative analysis in Section 4.8 that changes, which are visible in canopy height models, can be reliably detected using the developed method. Unfortunately, the changes below the canopy could not be validated. Also, only a weak agreement could be established by matching removed trees identified in different time periods (Section 4.7). Here, only large removed trees could be matched with a high accuracy and only less than halve of the small trees could be matched. The tree-to-tree matching here is influenced by both the detection of trees and the matching procedure. In particular over- and under-segmentation errors, but also the applied threshold on the degree of change as well as real physical changes influence the classification and position estimation of trees and result in difficulties to match trees. Similarly, in the validation by manual manipulation an increase in the threshold on the degree of change resulted in an increase in distances between matched trees. The evidence suggests that the tree-to-tree matching with the use of the horizontal distance between tree positions is not sufficiently robust.

How can changes in forests be detected efficiently and reliably using high density ALS data?

Changes in forest can be detected efficiently and reliably from high density ALS data using an approach that works on individual points in the three-dimensional space. This can be done with the methodology that has been presented in this thesis and consists of tree steps. First, deviating points are identified using an adapted cloud-to-cloud comparison, that is robust and adapts to density variations. Secondly, the deviating points are extracted and clustered into spatially connected regions that can be classified in the last step. In this way the available information is effectively exploited and reliable results can be obtained. Further, the computational efficiency is improved by using a kd -tree for the first processing step that considers all points. At later steps only subsets of the whole data set need to be processed. In this way the full data can be processed in a tolerable amount of time.

The results of this thesis can be compared to previous studies on the detection of harvested trees that are mentioned in Section 2.3. For example, Yu et al. (2004) automatically detected 61 out of 83 harvested trees by differencing canopy height models from 1998 and 2000 data with densities of 10 points/m². The method successfully detected all mature

harvested trees, but could not detect small trees. [Vastaranta et al. \(2012\)](#) differenced canopy height models of 2006 and 2010 to map snow induced canopy damage and obtained rates of omission errors between 19% and 75% per plot and rates of commission errors between 0% and 25%. The method was only suitable for dominant and codominant trees if dense point cloud data is available. These examples show that the new method, with measured overall accuracies of 65%, or 94% if adapting a parameter, and an omission error of 0%, can compete with the other methods.

The novelty of the presented method compared to other studies is the use of an approach based on individual points for change detection in forests, which thus takes full advantage of the three-dimensional information in ALS data. In this way not only large harvested and fallen tree can be identified, but also changes below the canopy surface. The method further has the potential to identify removed branches or changes in the foliation stage. Similar to the other studies the strongest limitation on the detection quality is the effect of over- and under-segmentation of trees. All in all, it is clear that the potential of the three-dimensional nature can be better exploited by considering each individual point of the data.

5.2 Recommendations

The developed method is very novel for forestry applications. Therefore several recommendation for further research can be made. First of all several improvements and alterations can be made to the method. Difference between data sets could alternatively be identified using a voxel based approach. Such an approach would most certainly improve the computational performance, but on the other hand might lack the amount of detail of the presented method. Another alternative would be to explicitly consider the shape of the local point distribution at the location of the query point. This could be combined with voxels for computational reasons.

Further it is recommended to improve the individual tree delineation approach. It is advised to not limit the merging of clusters by the horizontal distance between cluster centroids as this can lead to over- or under-segmentation of trees in the horizontal plane. An alternative solution is to use the maximum height at that location, which can be locally extracted using a canopy height model, and the vertical expansion of the clusters to decide whether two clusters can be merged. Such an approach should be closely linked to the classification step, which should include more relevant parameters and should be based on supervised learning. In addition, it should be investigated whether the whole region growing step can be replaced by the usage of voxels, such that the cluster merging, or in that case voxel merging, can be performed on a three-dimensional grid.

For the analysis of the results it is advised to develop a tree-to-tree matching approach that works in three dimensions in order to improve the matching performance. Additionally, commission errors can be simply avoided by inspection of the average degree of change in each detected cluster.

It is recommended for future research to investigate under which conditions the method works well and under which not. The first variable to consider is the point density. Which minimum point density is required in order to provide good results? Further the influence

of natural setting might have an impact on the result. Influential variables could be the type of forest, such as coniferous forests or rainforests, the density of trees, the age of the forest and the dynamics in the forest. In addition it is important to assess whether data sets with larger time span can be compared.

In this thesis the focus was on the detection of harvested trees, but it was shown that the method is capable of identifying smaller changes. Therefore more attention should be also paid to the analysis of small changes, such as broken branches, changes in foliation and also growth. This is where the method could unfold its full potential. However, since it appears that the distribution of the small changes can be extremely noisy it is suggested to first delineate all trees in the data set and then analyse which parts of each individual tree have changed and by how much they have changed. For the modelling of growth it must be clarified how the degree of change or a similar parameter can be related to the real magnitude of change. After the exploration of these potential capabilities it would be possible to conclude if and how this or a similar approach can be used for other ecological studies, such as canopy gap dynamics.

Point density is an important factor in order to detect changes. The higher the point density the smaller the detectable change is. High point density data in forestry studies are however still rare, but it can be expected that the point densities will increase in the future. It is therefore important to further explore the potential of high density ALS data and develop data management tools to store and analyse the data within tolerable times. The data sets of the Kralingse Bos, provided by the Municipality of Rotterdam, have proven to be useful for experimentation with high density ALS data in forest environments. In addition to the used data, the AHN2 and the new 2014 data could be used. This data collection resembles an unprecedented collection of high density ALS data in both urban and forest environments and could be used for further research. With the available data sets also more attention can be directed onto the creation and analysis of time series.

References

- Barber, D. M., Holland, D., and Mills, J. P. (2008). Change detection for topographic mapping using three-dimensional data structures. *The International Archives of the Photogrammetry, Remote Sensing and Spatial Information Sciences*, XXXVII. Part B4.
- Bremer, M., Wichmann, V., and Rutzinger, M. (2013). Eigenvalue and graph-based object extraction from mobile laser scanning point clouds. *ISPRS Annals of Photogrammetry, Remote Sensing and Spatial Information Sciences*, 1(2):55–60.
- Bucksch, A., Lindenbergh, R., Abd Rahman, M., and Menenti, M. (2014). Breast height diameter estimation from high-density airborne lidar data. *Geoscience and Remote Sensing Letters, IEEE*, 11(6):1056–1060.
- FAO (2010). Global forest resources assessment 2010: main report. *FAO Forestry Paper*, 163:340.
- Friedman, J. H., Bentley, J. L., and Finkel, R. A. (1977). An algorithm for finding best matches in logarithmic expected time. *ACM Transactions on Mathematical Software*, 3(3):209–226.
- Girardeau-Montaut, D., Roux, M., Marc, R., and Thibault, G. (2005). Change detection on points cloud data acquired with a ground laser scanner. *International Archives of Photogrammetry, Remote Sensing and Spatial Information Sciences*, 36(part 3):W19.
- Hu, B., Li, J., Jing, L., and Judah, A. (2014). Improving the efficiency and accuracy of individual tree crown delineation from high-density lidar data. *International Journal of Applied Earth Observation and Geoinformation*, 26(0):145 – 155.
- Hyypä, J., Hyypä, H., Leckie, D., Gougeon, F., Yu, X., and Maltamo, M. (2008). Review of methods of smallfootprint airborne laser scanning for extracting forest inventory data in boreal forests. *International Journal of Remote Sensing*, 29(5):1339–1366.
- Kaartinen, H., Hyypä, J., Yu, X., Vastaranta, M., Hyypä, H., Kukko, A., Holopainen, M., Heipke, C., Hirschmugl, M., Morsdorf, F., Nsset, E., Pitknen, J., Popescu, S., Solberg,

- S., Wolf, B. M., and Wu, J.-C. (2012). An international comparison of individual tree detection and extraction using airborne laser scanning. *Remote Sensing*, 4(4):950–974.
- Lee, H., Slatton, K. C., Roth, B. E., and Cropper, W. P. (2010). Adaptive clustering of airborne lidar data to segment individual tree crowns in managed pine forests. *International Journal of Remote Sensing*, 31(1):117–139.
- Leeuwen, M. and Nieuwenhuis, M. (2010). Retrieval of forest structural parameters using lidar remote sensing. *European Journal of Forest Research*, 129(4):749–770.
- Lim, K., Treitz, P., Wulder, M., St-Onge, B., and Flood, M. (2003). Lidar remote sensing of forest structure. *Progress in Physical Geography*, 27(1):88–106.
- Lindenbergh, R. and Pietrzyk, P. (2015). Change detection and deformation analysis using static and mobile laser scanning. *Applied Geomatics*, pages 1–10.
- MATLAB (2014). *version 8.3.0.532 (R2014a)*. The MathWorks Inc., Natick, Massachusetts.
- McRoberts, R., Bollandss, O., and Nsset, E. (2014). Modeling and estimating change. In Maltamo, M., Nsset, E., and Vauhkonen, J., editors, *Forestry Applications of Airborne Laser Scanning*, volume 27 of *Managing Forest Ecosystems*, pages 293–313. Springer Netherlands.
- Morsdorf, F., Meier, E., Allg, B., and Daniel, N. (2003). *Clustering in airborne laser scanning raw data for segmentation of single trees*, volume XXXIV-3/W1, pages 1–7.
- Næsset, E. and Gobakken, T. (2005). Estimating forest growth using canopy metrics derived from airborne laser scanner data. *Remote Sensing of Environment*, 96(34):453 – 465.
- Nyström, M., Holmgren, J., and Olsson, H. (2013). Change detection of mountain birch using multi-temporal als point clouds. *Remote Sensing Letters*, 4(2):190–199.
- Pietrzyk, P. and Lindenbergh, R. (2014). Detection of harvested trees in forests from repeated high density airborne laser scanning. *ISPRS Annals of Photogrammetry, Remote Sensing and Spatial Information Sciences*, pages 275–280.
- Popescu, S. C. and Zhao, K. (2008). A voxel-based lidar method for estimating crown base height for deciduous and pine trees. *Remote Sensing of Environment*, 112(3):767 – 781.
- Puttonen, E. and Litkey, P. (2014). *Matlas tools: A mex Gateway for Utilizing lastools Read and Write Functions in MATLAB*. Finnish Geodetic Institute.
- Rahman, M. and Gorte, B. (2008). Individual tree detection based on densities of high points of high resolution airborne lidar. *GEOBIA*, pages 350–355.
- Reitberger, J., Schnörr, C., Krzystek, P., and Stilla, U. (2009). 3d segmentation of single trees exploiting full waveform lidar data. *ISPRS Journal of Photogrammetry and Remote Sensing*, 64(6):561 – 574.

- Richter, R., Kyprianidis, J. E., and Dllner, J. (2013). Out-of-core gpu-based change detection in massive 3d point clouds. *Transactions in GIS*, 17(5):724–741.
- Shan, J. and Toth, C. K. (2008). *Topographic laser ranging and scanning: principles and processing*. CRC Press.
- Vastaranta, M., Korpela, I., Uotila, A., Hovi, A., and Holopainen, M. (2011). Area-based snow damage classification of forest canopies using-temporal lidar data. *ISPRS-International Archives of the Photogrammetry, Remote Sensing and Spatial Information Sciences*, 3812:169–173.
- Vastaranta, M., Korpela, I., Uotila, A., Hovi, A., and Holopainen, M. (2012). Mapping of snow-damaged trees based on bitemporal airborne lidar data. *European Journal of Forest Research*, 131(4):1217–1228.
- Vauhkonen, J., Ene, L., Gupta, S., Heinzl, J., Holmgren, J., Pitkänen, J., Solberg, S., Wang, Y., Weinacker, H., Hauglin, K. M., et al. (2011). Comparative testing of single-tree detection algorithms under different types of forest. *Forestry*, page cpr051.
- Vauhkonen, J., Maltamo, M., McRoberts, R. E., and Næsset, E. (2014). Introduction to forestry applications of airborne laser scanning. In *Forestry Applications of Airborne Laser Scanning*, pages 1–16. Springer.
- Vepakomma, U., Kneeshaw, D., and Fortin, M.-J. (2012). Spatial contiguity and continuity of canopy gaps in mixed wood boreal forests: persistence, expansion, shrinkage and displacement. *Journal of Ecology*, 100(5):1257–1268.
- Vepakomma, U., Kneeshaw, D., and St-Onge, B. (2010). Interactions of multiple disturbances in shaping boreal forest dynamics: a spatially explicit analysis using multi-temporal lidar data and high-resolution imagery. *Journal of Ecology*, 98(3):526–539.
- Vepakomma, U., St-Onge, B., and Kneeshaw, D. (2008). Spatially explicit characterization of boreal forest gap dynamics using multi-temporal lidar data. *Remote Sensing of Environment*, 112(5):2326 – 2340. Earth Observations for Terrestrial Biodiversity and Ecosystems Special Issue.
- Vosselman, G. and Maas, H.-G. (2010). *Airborne and Terrestrial Laser Scanning*, volume XXXVI. CRC Press.
- Wallace, L., Lucieer, A., and Watson, C. S. (2014). Evaluating tree detection and segmentation routines on very high resolution uav lidar ata. *IEEE Transactions on Geoscience and Remote Sensing*, 52(12):7619–7628.
- Wehr, A. and Lohr, U. (1999). Airborne laser scanningan introduction and overview. *ISPRS Journal of Photogrammetry and Remote Sensing*, 54(23):68–82.
- Yu, X. (2008). Methods and techniques for forest change detection and growth estimation using airborne laser scanning data.
- Yu, X., Hyypä, J., Kaartinen, H., and Maltamo, M. (2004). Automatic detection of harvested trees and determination of forest growth using airborne laser scanning. *Remote Sensing of Environment*, 90(4):451 – 462.

- Yu, X., Hyypä, J., Kukko, A., Maltamo, M., and Kaartinen, H. (2006). Change detection techniques for canopy height growth measurements using airborne laser scanner data. *Photogrammetric Engineering and Remote Sensing*, 72(12):1339.

Appendix A

Point Clouds of Sample Area

The raw point clouds of the sample area that were used for processing are depicted in the Chapter. In Figure A.1 the point cloud of the year 2008 can be seen. Figures A.2 and A.1 show the point clouds of the years 2010 and 2012, respectively. Clear differences in the foliation state can be seen between the 2010 data and the other two. Also a small amount of growth is visible from 2008 to 2012.

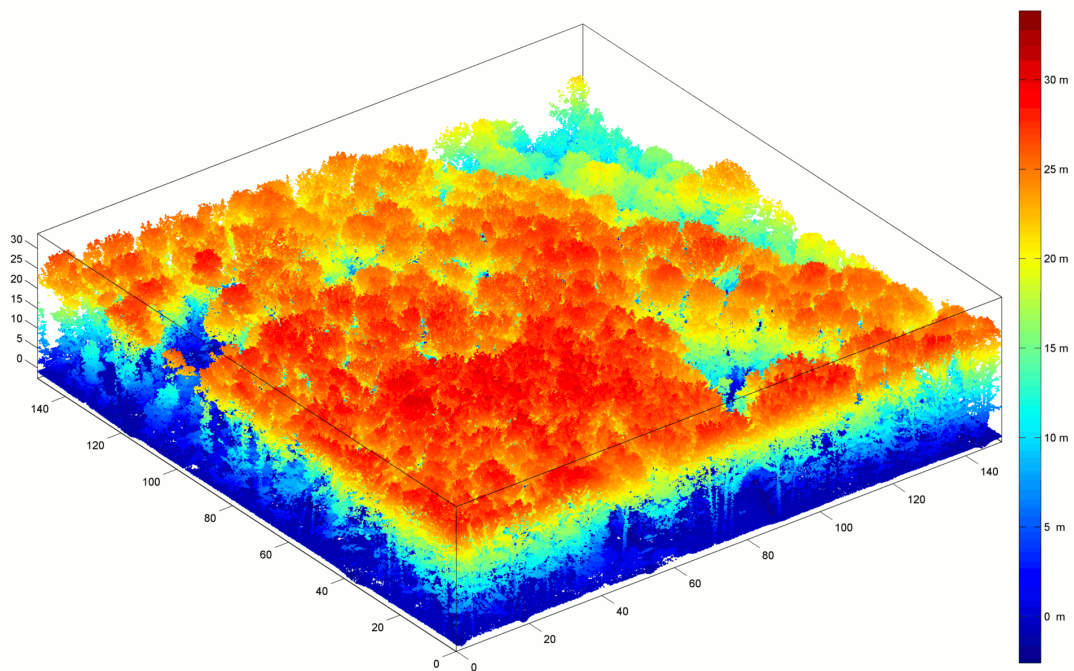


Figure A.1: 2008 point cloud of sample area coloured by elevation above mean sea level.

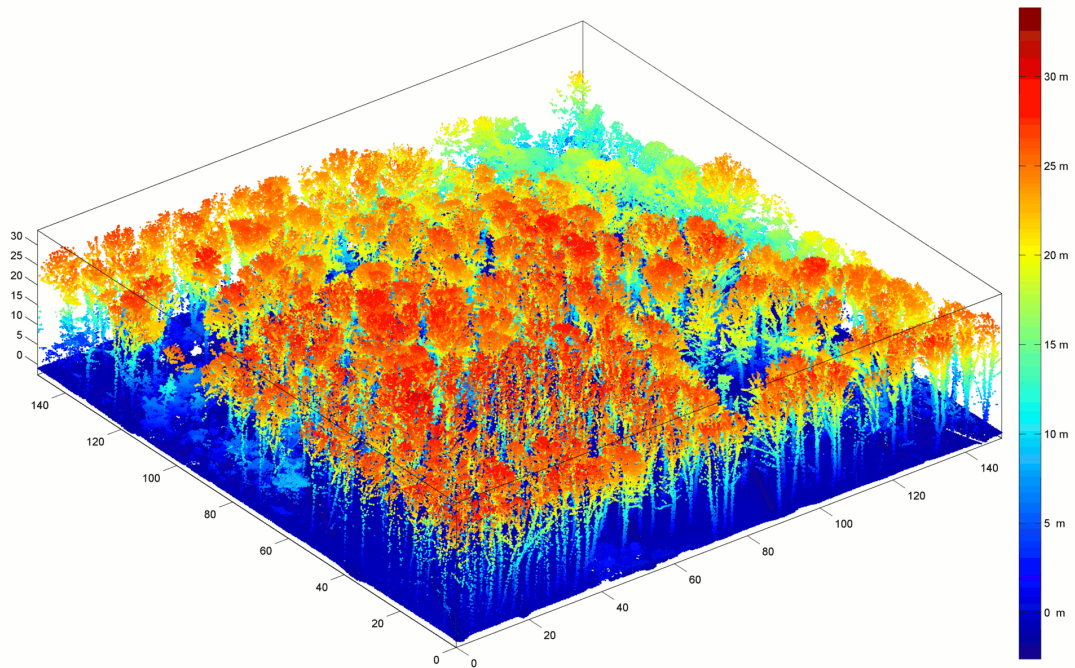


Figure A.2: 2010 point cloud of sample area coloured by elevation above mean sea level.

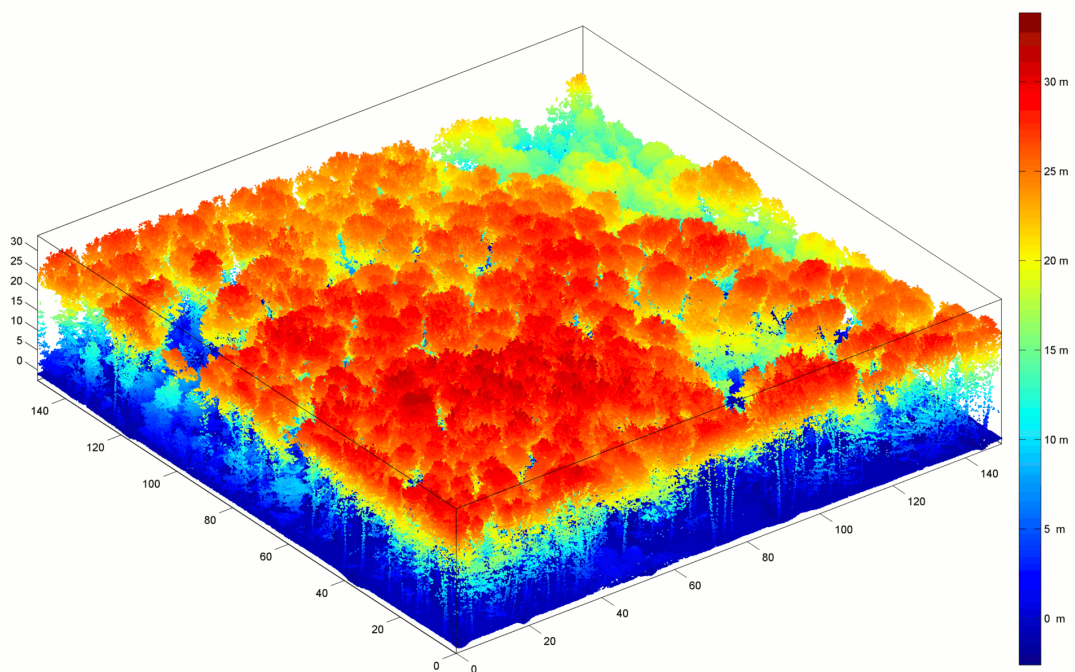


Figure A.3: 2012 point cloud of sample area coloured by elevation above mean sea level.